Nanotechnology for diagnosis and therapy of rheumatoid arthritis: evolution towards theranostic approaches

Junkai Zhao[a,#], Xuan Chen[a,#], Kwun-Hei Ho[b], Chao Cai[a], Cheuk-Wing Li[c], Mo Yang[b,*], Changqing Yi[a,*]

[a] *Guangdong Provincial Key Laboratory of Sensor Technology and Biomedical Instrument, School of Biomedical Engineering, Sun Yat-Sen University, Shenzhen 518107, P. R. China.*
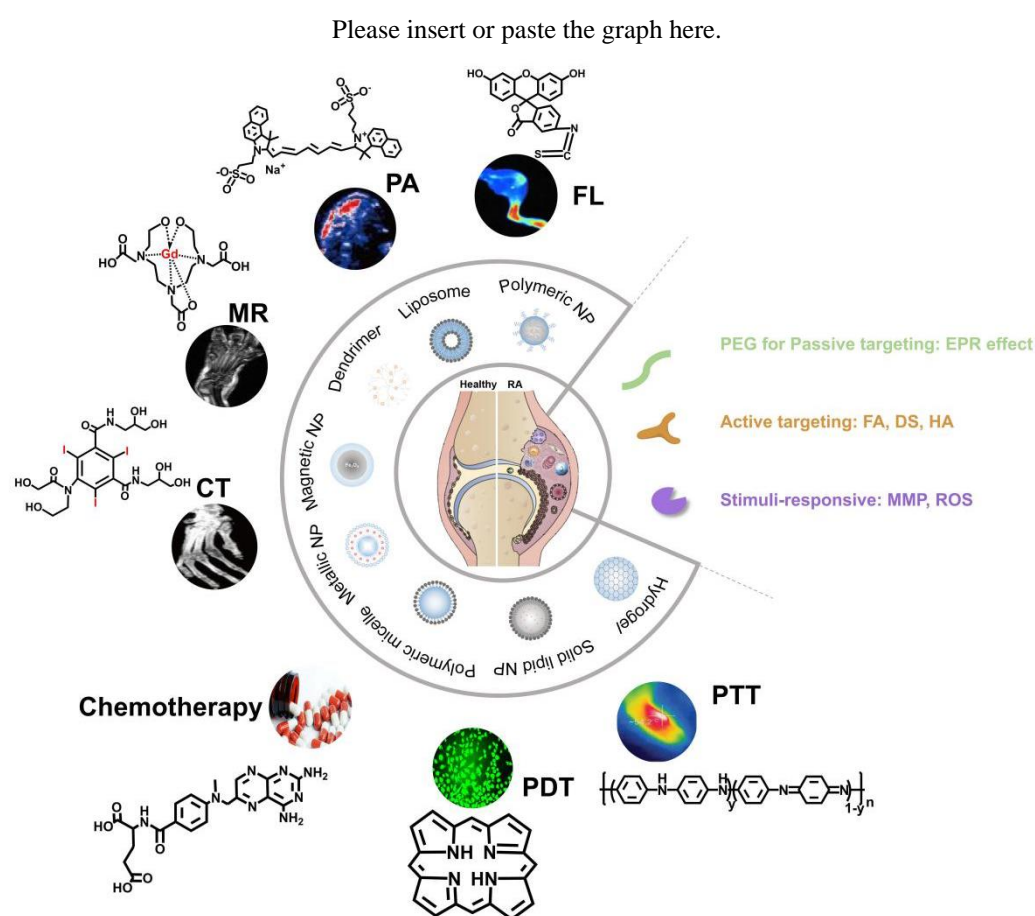
[b] *Department of Biomedical Engineering, the Hong Kong Polytechnic University, Hong Kong, P. R. China.*

[c] *School of Science and Technology, Nottingham Trent University, Clifton Lane, Nottingham, NG11 8NS, United Kingdom.*

[*] *Corresponding authors: C. Q. Yi, Email: yichq@mail.sysu.edu.cn; Tel: 86-20-39342380.*

M. Yang, Email: mo.yang@polyu.edu.hk; Tel: 852-9065 8264.

[#] *These authors contributed equally to this work.*

Please insert or paste the graph here.

This review summarizes the nano diagnosis and nanotherapy of rheumatoid arthritis, and discusses the application of nanotheranostic in RA.

Nanotechnology for diagnosis and therapy of rheumatoid arthritis: evolution towards theranostic approaches

Junkai Zhao[a, #], Xuan Chen[a, #], Kwun-Hei Ho[b], Chao Cai[a], Cheuk-Wing Li[c], Mo Yang[b, *], Changqing Yi[a, *]

[a] Guangdong Provincial Key Laboratory of Sensor Technology and Biomedical Instrument, School of Biomedical Engineering, Sun Yat-Sen University, Shenzhen 518107, P. R. China.
[b] Department of Biomedical Engineering, the Hong Kong Polytechnic University, Hong Kong, P. R. China.
[c] School of Science and Technology, Nottingham Trent University, Clifton Lane, Nottingham, NG11 8NS, United Kingdom.
[*] Corresponding authors: C. Q. Yi, Email: yichq@mail.sysu.edu.cn; Tel: 86-20-39342380.
M. Yang, Email: mo.yang@polyu.edu.hk; Tel: 852-9065 8264.
[#] These authors contributed equally to this work.

ARTICLE INFO

ABSTRACT

Rheumatoid arthritis (RA), as a chronic autoimmune disease, damages the bone and cartilage of patients, and even leads to disability. Therefore, the diagnosis and treatment of RA is particularly important. However, due to the complexity of RA, it is difficult to make an effective early diagnosis of RA, which is detrimental to RA treatment. Besides, long-term intake of anti-RA drugs can also cause damage to patients' organs. The emergence of nanotechnology provides the new train of thoughts for the diagnosis and treatment of RA. And the combination of diagnosis and therapy is an ideal method to solve the problem of disease management of RA patients. In this review, we summarized the mechanism and microenvironment of RA lesions, the commonly used diagnostic techniques and therapeutic drugs of RA, and review their advantages and disadvantages. New nanotherapy strategies such as drug-carrying nanoparticles, PTT, PDT are listed, and their applications in RA treatment is summarized. In addition, multimodal imaging, combined therapy and responsive diagnosis and treatment are also summarized as important contents. At last, we also review some typical nanocarriers that can be used in the integration of diagnosis and therapy, and discussed their potential applications in RA.

1   Introduction

1.1. Overview of rheumatoid arthritis（RA）

Rheumatoid arthritis (RA) is a progressive autoimmune disease which causes chronic, systemic inflammatory disorder with initial symptoms such as joint pain and swelling in the hands and feet. The high morbidity and mortality rate of RA were reported with global prevalence about 0.5-1% [1]. Typically, the onset age of RA is around 40 to 50 years old with female to male ratio from 2:1 to 3:1 [2]. There are several risk factors that may cause RA, including various immune components, genetic sensitivity, disorder of sexual hormones, infection and environment factors. RA affects most of the joints in human body, including small joints of hands, wrists, elbows, knees, ankles and feet [3]. As a consequence of extra-articular immunologic response, RA may also induce damage to other organs such as the heart, lungs, eyes, skin and blood vessels. If RA is remained untreated, the progressive damage could lead to severe functional deterioration or even fatality [4]. Therefore, it is very important to develop effective strategies for diagnosis and treatment of RA to prevent joint destruction, long-term disability and complications. In fact, a major breakthrough in RA disease management is early diagnosis and appropriate treatment, which can substantially improve patient functional outcomes and lower the morbidity rate [5].

Although the pathogenesis of RA is not completely understood, it is generally considered that inflammation starts from the synovium with intimal hyperplasia. This results in superficial layer of macrophage-like synoviocytes (MLS) and fibroblast-like synoviocytes (FLS) which overlies the interstitial zone (**Fig. 1**) [2]. The interstitial zone consists of marked cellular infiltrate, macrophages, synovial fibroblasts, mast cells, B-cells, T-cells and plasma cells. The primary function of B cells is to differentiate into plasma cells that produce two most important autoantibodies: anti-citrullinated peptide /protein antibody (ACPA) and rheumatoid factor (RF) [6, 7]. On the other hand, pro-inflammatory cytokines such as IL-1β, TNF-α and IL-6 will be overproduced by fibroblast-like cells and macrophages *via* activation of T cells [8]. In addition, TNF-α and tissue degrading matrix metalloproteases (MMPs) which are able to stimulate the development of osteoclasts for bone abrasion, will be released by synovial cells upon the induction of both macrophages and fibroblast-like cells [2]. Consequently, this vicious cycle results in activation of more macrophages, lymphocytes, and fibroblasts cells which lead to continuous RA inflammatory process [8]. The inflammatory cytokines such as TNF-α, IL-1, IL-6, IL-8, IL-17, MMPs and granulocyte colony-stimulating factor (G-CSF) are rich in the synovial fluid and synovium of RA patients. All these inflammatory cytokines play key roles in the progress of inflammation, cartilage degradation, and bone loss [2, 9, 10] through inducing vascular endothelial growth factor (VEGF) and receptor activator of nuclear factor β ligand (RANKL). RANKL can regulate osteoclastogenesis, which affects osteoclast signaling, and thereafter directly causes bone destruction process [11]. And VEGF can stimulate angiogenesis and recruit more inflammatory leukocytes to keep inflamation.
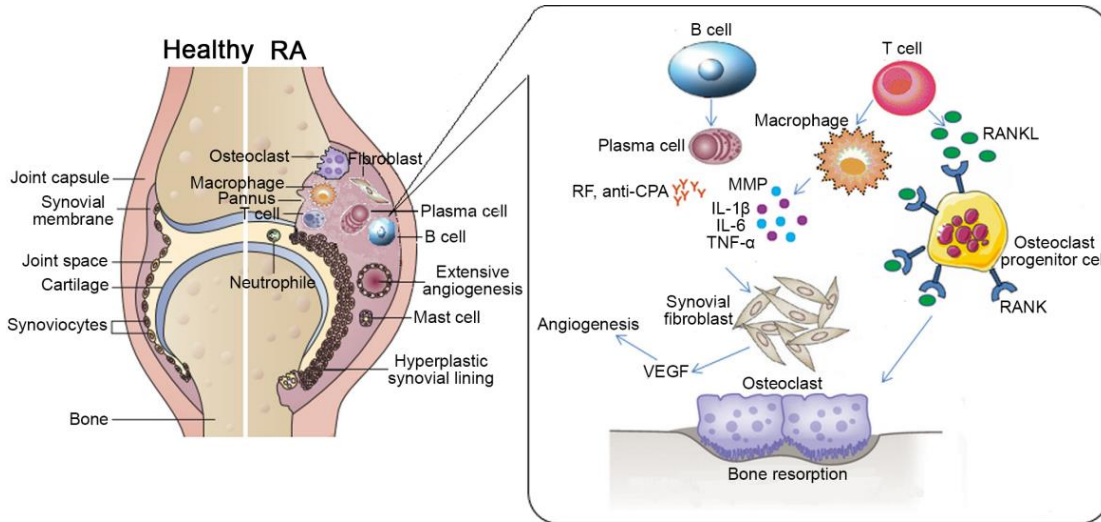
Fig. 1. Pathogenesis of RA. Copied with permission [2]. Copyright 2016, Elsevier Masson SAS.

1.2. Current diagnosis and treatment strategies for RA

In clinical practices, clinicians currently are recommended to use the RA classification standard issued by the ACR in 1987 [12] and the ACR/EULAR in 2010 [13] for diagnosis. However, such diagnosis is largely based on physical check and observation of characteristic symptoms, such as pain, stiffness and swelling of multiple joints in bilaterally symmetrical patterns [14]. This means that pure clinical diagnosis can only be confirmed after half to one year of RA development, making early diagnosis of RA almost impossible. In addition, the symptoms and pathological features of RA are usually non-specific, leading to low clinical, radiological or immunological diagnosis efficiency and absence of gold standard approach for RA diagnosis [15]. In view of this, Chinese Rheumatology Association formulated the 2018 Chinese guideline for the diagnosis and treatment of RA (hereafter referred as 'guideline') [16]. The 2018 guideline states that clinicians need to make diagnosis based on the patient's clinical manifestations, laboratory and imaging examinations (**Fig. 2**) [16].
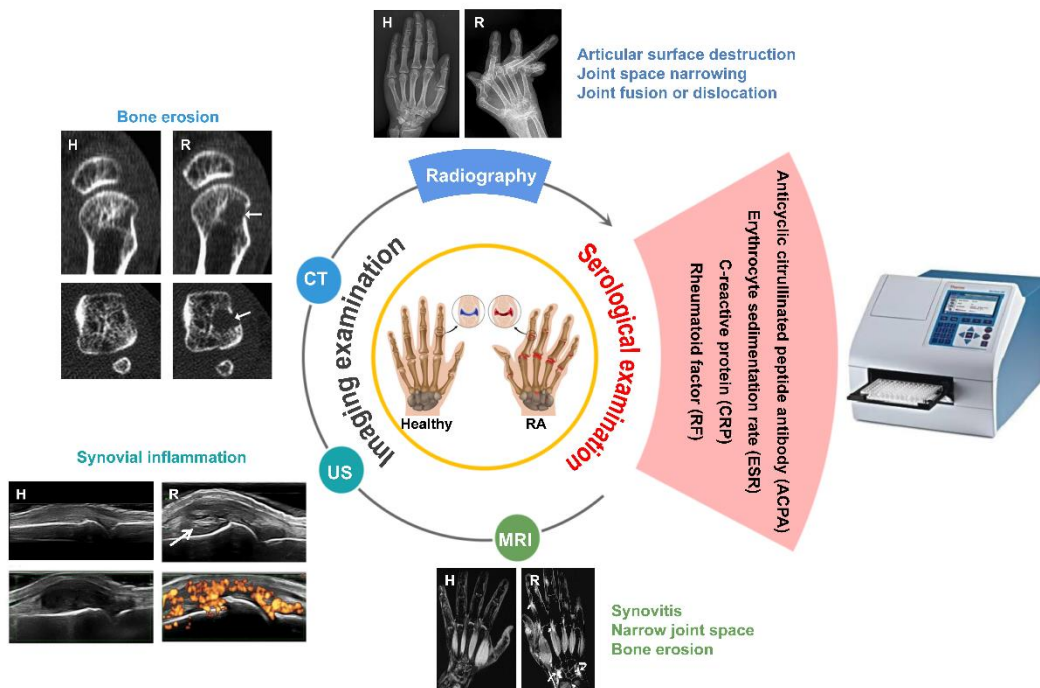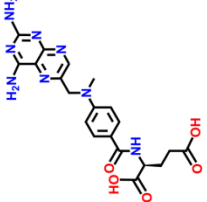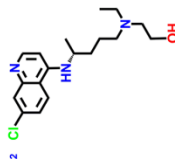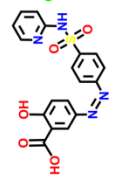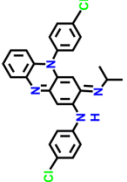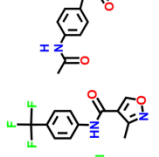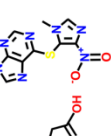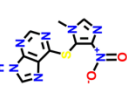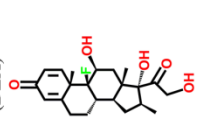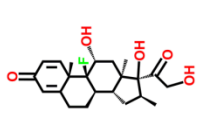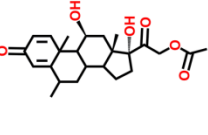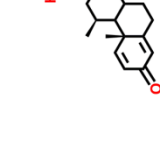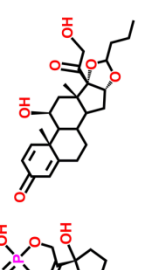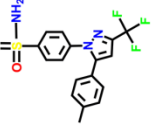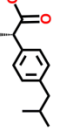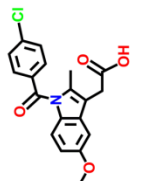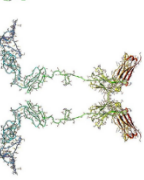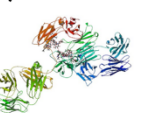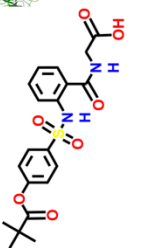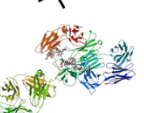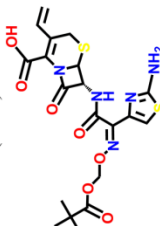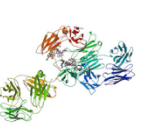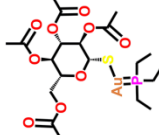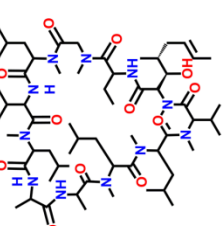

Fig. 2. RA diagnostic techniques used in clinic. H, healthy; R, RA.

Serological tests are used to detect various biomarkers in blood including antibodies (RF, ACPA) due to the immune-response and/or acute phase reactants (C-reactive protein (CRP), erythrocyte sedimentation rate (ESR)) that are elevated during inflammatory condition. If at least one of RF and ACPA exhibits a positive titer and an increased level of an acute phase reactant (CRP or ESR) is observed, the patient may be diagnosed with RA [13].

Table 1
Current therapeutic agents for RA.

Classification	Instance	Mechanism of action	Side effects
DMARDs	Methotrexate (MTX), Hydroxychloroquine (HCQ), Sulfasalazine (SSZ), Clofazimine (CLO), Leflunomide (LEF), Actarit, Azathioprine	Immunosuppression, inhibition of genetic.	Hepatic cirrhosis, myelosuppression, interstitial pneumonitis, gastrointestinal disorders, etc.
GCs	Dexamethasone (DEX), Betamethasone, Methylprednisolone acetate, Prednisolone phosphate, Budesonide	Prevention of phospholipid release, anti-inflammation, immunosuppression.	Insulin resistance, hyperadrenocorticism, infection, hypertension and atherosclerosis, osteoporosis and osteonecrosis, obesity, skin thinning and inhibition of wound repair, etc.
NSAIDs	Aspirin, Celecoxib, Ibuprofen, Indomethacin	Inhibition of COXs, reduce acute inflammation, analgesia.	Gastrointestinal disturbance, renal malfunction, increase cardiovascular risk, etc.
Biological agents	Etanercept (ETA), Infliximab (IFX), Adalimumab (ADA), Golimumab (GOL), Anakinra (AKR), Tocilizumab (TCZ)	Antagonism of TNF-α, IL-1 receptor, or IL-6 receptor.	Infection, tuberculosis reactivation, gastrointestinal perforation.
	Auranofin, Cyclosporine, Rituximab (RIT)	Reduce the formation of RF and antibody, downregulate T cells activation, deplete B-cell.	Infection, hypersensitivity, hypertension, renal disease, respiratory difficulty, diarrhea.

The imaging diagnostic methods for RA include conventional radiography, ultrasonography (US), computed tomography (CT) and magnetic resonance imaging (MRI). The imaging diagnostic criteria for RA are based on the size and number of affected joints and the duration of synovitis. RA patients should meet the criteria of being involved with medium or large joint ≥2, or being involved with small joint ≥1, or the duration of synovitis being larger than 6 weeks [13]. Among various imaging approaches, conventional radiography such as X-ray is the most commonly used imaging tool for assessing RA joint structural damage. The conventional radiography images of healthy subjects show integral baseline joint, the cortical bone has a clear margin [17]. The margin of joints of RA patients may be interrupted if an erosion is present or become more closely apposed to an adjacent cortex if the joint is narrowed. The X radiographs of

early RA showed periarticular soft tissue swelling, and periarticular or juxta-articular osteoporosis; as the disease progresses, articular surface destruction, joint space stenosis, joint fusion or dislocation may occur [16]. X-ray can visualize articular surface destruction, joint space narrowing, juxta-articular osteoporosis, cysts and joint fusion or dislocation in severe cases, but it is not able to detect early disease manifestations such as soft tissue changes and bone erosion [16]. Although X-rays are convenient and cheap, they suffer from danger of radiation and poor sensitivity for early diagnosis.

CT is able to detect destruction of calcified tissue such as bone erosions in RA and realize 3D visualization of joints [18]. This can improve the detection sensitivity of erosions, especially at complex sites such as the wrist, so as to assist diagnosis as early as possible. Healthy subject does not reveal any erosions at the metacarpal head, while metacarpophalangeal (MCP) joints of RA patient show obvious erosion. In addition, the status of appendicular skeleton of RA patients can be evaluated by CT techniques such as dual energy CT and high-resolution CT [19, 20]. However, CT is radiant, expensive and unable to detect active inflammations such as synovitis and tenosynovitis.

US is convenient and inexpensive for evaluation of the synovial, bone, and cartilage structures of multiple joints and monitoring of synovial inflammation. Compared with conventional radiographic examination, US is more sensitive in detecting joint structural damage, which can clearly show the thickness and morphology of synovium, synovial sac, articular cavity effusion and articular cartilage [21]. In addition, US can also dynamically determine the amount of joint effusion and the distance from the body surface to guide joint puncture and treatment. The US images of healthy subjects show that neither synovial hypertrophy independently of the presence of effusion nor Doppler activity can be observed [22]. If the synovial hypertrophy with or without effusion is up to the level of horizontal line connecting bone surfaces metacarpal head and proximal phalangeal bone, but with upper surface flat or convex (curved downwards), the person may suffer RA with appearance of Doppler signals. The severity is determined by grey-scale-detected synovial hypertrophy and power Doppler signal (within the synovium) strength [22]. Doppler ultrasound can be used to confirm the presence of synovitis, to monitor disease activity and progression, and to assess inflammation [23, 24]. However, US is extremely dependent on the skills of the operator.

MRI is the most sensitive tool for diagnosis of early RA lesions such as synovitis, joint space narrowing and bone erosion, but suffers from the high cost [25]. The synovial thickening, bone marrow edema and slight articular surface erosion can be found in early RA by MRI, which is significant for the early diagnosis of RA. Compared with normal subjects, the MR signal intensity of synovial compartment in RA patients was enhanced after gadolinium injection and the MR signal intensity of cortical bone was increased, while trabecular bone signal was decreased [26]. The detection of early inflammation by MRI and US is superior to that of clinical examination. It can be used to predict not only whether undifferentiated arthritis will develop into RA, but also to predict future joint damage in clinical remission to evaluate the incidence of persistent inflammation. However, due to the difficulties in the confirmation of characteristic symptoms at its early stage, early diagnosis of RA is still challenging.

In terms of treatment, the 2018 guideline states that the treatment principle of RA is early standardized therapy with regular monitoring and follow-up. Inhibiting the production and action of cytokines as early as possible can effectively prevent or slow down the joint synovitis and cartilage lesions, ultimately control the disease condition, reduce the disability rate and ultimately improve the life quality of patients. The RA treatment methods have been constantly optimized over the continuous research of years. Currently, there are four basic categories of therapeutic agents for RA, namely disease-modifying anti-rheumatic drugs (DMARDs), glucocorticoids (GCs), non-steroidal anti-inflammatory drugs (NSAIDs), and biological agents, as summarized in **Table 1** [2, 27, 28].

Methotrexate (MTX) is a typical DMARD and reckoned as a first-line drug for RA treatment since early 1980s which can be used alone or in combination with other drugs. GCs can interfere the macrophage accumulation and weaken capillary permeability, therefore, they are mostly utilized for the initial treatment of critically active RA. NSAIDs lead to remission of inflammation-related symptoms by suppressing the production of prostaglandin. Biological agents, for example, infliximab (INF), etanercept (ETA), and tocilizumab (TCZ) can block IL-6 receptor or inhibit TNF-α, which have attributed to the revolutionized RA therapy in clinic. Although these treatments are effective, their usage is limited due to their damaging side effects, such as cardiac complications, ulcers and gastrointestinal damage, along with immune-suppression that lead to the development of opportunistic infections [27]. Therefore, there is an urgent need to propose safer and more effective approaches for RA treatment.

1.3. Superiorities of nanotechnology for RA diagnosis and therapy

Nowadays, nanomaterial is booming, and their applications in biomedicine including diagnostics and therapy are dramatically growing due to its high drug loading efficiency, multi-modality imaging capability, passive and/or active targeting effects. By using the nanoscale drug-carriers, therapeutic or imaging agents can be selectively delivered to the desired inflammation site in a controlled or sustained manner. In this way, therapeutic effects of traditional anti-RA drugs can be substantially enhanced, and their side effects induced by short biological half-life and poor bioavailability can be obviously lowered [29]. More importantly, nanomaterials provide a robust framework in which more than one therapeutic and/or imaging agents can be incorporated to offer synergetic multifunctional nanomedicine. Various mild conjugation strategies have been well established for the linkage of therapeutic and/or imaging agents onto the surface of nanomaterials [30]. Actually, nanomaterials are extensively used to unite diagnostic molecules and drugs into a single agent [31].

Nanotheranostic is able to provide specific targeting, non-invasive imaging, and effective therapy at the lesion sites without affecting surrounding healthy cells [32, 33]. Generally, nanotheranostic probe is consisted of several functional components: diagnostic contrast agents, therapeutic moieties, targeting moieties, and some surface modification or coating moieties that improve the bio-compatibility and water solubility. **Fig. 3** illustrates the frequently used functional components in nanotheranostic probes for RA. Due to the combination of diagnosis and therapy in a single platform, nanotheranostic shows its remarkable advantages for RA diagnosis and treatment. Firstly, nanotheranostic makes early diagnosis of RA possible, which can subsequently facilitate early treatment of RA, and thereby improving the therapeutic effect. Secondly, monitoring during treatment may improve prognoses, thereby speeding up clinician's therapeutic decisions [34]. Thirdly, the introduction of targeting moiety will reduce the abuse of anti-RA drugs and cost of treatment.

The pursuit of new diagnostics and therapeutics for RA remains an open and hot research field. Nanotechnology represents a novel strategy for diagnosis and treatment of RA. This review summarizes the current development of nanoprobes for RA diagnostics and therapeutics. Special focus of this review is put on nanotheranostic which holds the promise for theranostic approaches to RA.
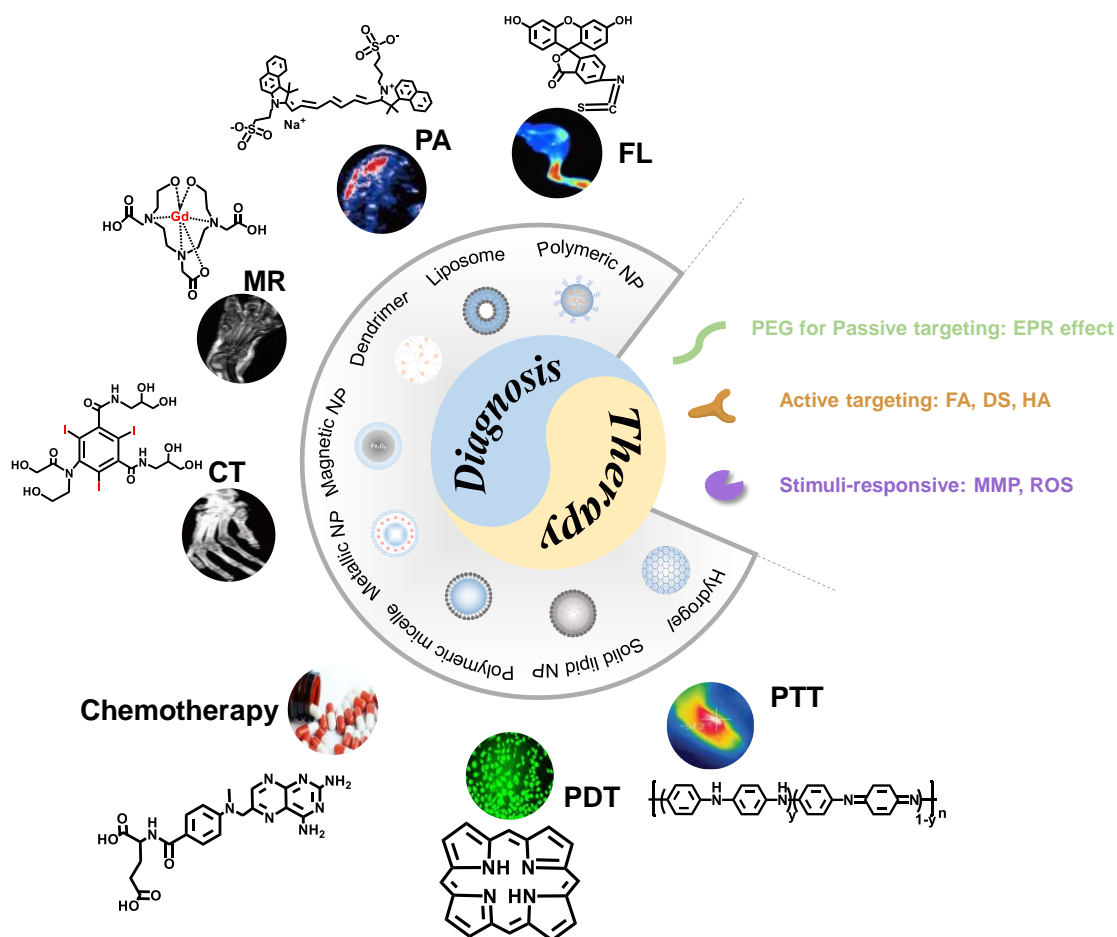
Fig. 3. The summary of the key components for RA theranostics.

2 Nanoparticle-based diagnostics for RA

The rapidly developed molecular imaging technology allows the clinicians to diagnose RA more accurately and quickly, because of its advantages such as non-invasive quantification of biological processes even at molecular level [35]. Molecular imaging technology can not only make early diagnosis of RA possible, but also evaluate the treatment effect and guide personalized RA therapy. Molecular probes with excellent performance are the basis of molecular imaging technology. **Table 2** summarizes frequently used contrast agents in clinic. However, these probes are generally nonspecific, and suffer from short half-life, easy to discharge, high dosage and strong toxicity. All of these limit the wide application of molecular imaging in accurate and effective diagnosis of RA.

It is well recognized that the performance of imaging probes can be substantially improved by integration with more functions. Therefore, the introduction of nanoprobes is beneficial to the application of molecular imaging in RA diagnosis. The nanoprobes have the advantages of good specificity, water solubility, excellent stability and biocompatibility *in vivo,* which make them have the potential to be used for early diagnosis of RA. In this section, in order to shed light on future design and applications of nanoscale imaging probes in RA diagnosis, superiority and limitation of nanoparticle-based diagnostics for RA will be discussed in detail.

2.1. MRI
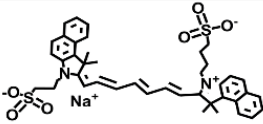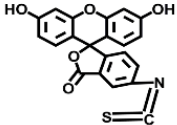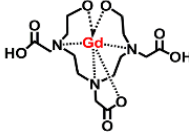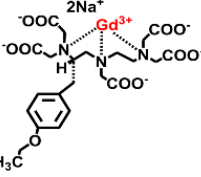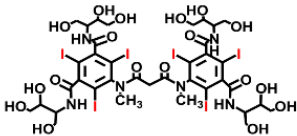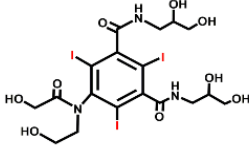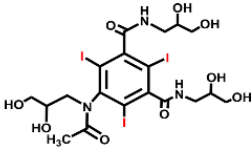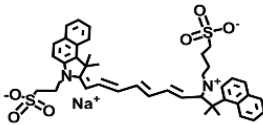
MRI refers to the use of the principle of nuclear magnetic resonance and gradient magnetic field to detect the radiation signal emitted by the human body, and then generate the internal structure image of the object. In clinical MRI, the presence of a large number of hydrogen atoms in the human body is often used to achieve imaging effects. MR imaging which uses the main magnetic field and RF magnetic field to image human tissues and organs, is a non-invasive imaging technique with high spatial and contrast resolution. During the imaging process, high-contrast clear images of human tissues and organs without ionizing radiation can be obtained, and the abnormalities and early pathological changes of human organs can be differentiated. Especially, MRI can acquire images of soft tissues at multiple directions and different properties, which can clearly show synovial lesions, bone edema, cartilage destruction in patients with early rheumatoid arthritis [36-38].

The use of contrast agents can significantly improve imaging quality of MRI. There are two categories of MR contrast agents according to the action principle, namely, longitudinal relaxation contrast agent (T_1 contrast agent) and transverse relaxation contrast agent (T_2 contrast agent). T_1 contrast agents are usually paramagnetic materials, which can directly react with the hydrogen nucleus in water molecules to shorten longitudinal relaxation time, thus enhancing the signal and brightening the image. Typical T_1 contrast agents used

in clinic include Gd-based contrast agents such as Gd-DTPA, Gd-DOTA, and etc., and Mn-based contrast agents such as Mn-DPDP, MnCl$_2$, and etc., because of the seven unpaired electrons of Gd^{3+} and five unpaired electrons of Mn^{2+} [39, 40]. However, these small molecular contrast agents suffer from poor selectivity and short half-life, resulting in weak signal *in vivo*. To address this issue, Hou et al designed a targeted MRI contrast agent CB86-DTPA-Gd for RA diagnosis by chelation of Gd^{3+} onto TSPO ligand CB86 modified DTPA. TSPO is considered as a suitable candidate biomarker for inflammatory diseases such as RA, because it plays a key role in macrophage regulation in inflammatory regions. After being injected into collagen-induced arthritis (CIA) mice, the signal-to-noise ratio of RA site was 2.49 times higher than that of Gd-DTPA group [41].

Table 2
The summary of typical contrast agents in clinic.

Imaging modality	Contrast agent	Structure	Properties	Superiority	Limitation
FLI	ICG	(structure)	E_m=835nm QY=13%	Excellent optical properties Good biocompatibility	Poor colloidal stability Short half-life Low cell uptake
	FITC	(structure)	E_m=520nm QY=30%~85%	High absorptivity Excellent fluorescence QY Good colloidal solubility	Poor colloidal stability
MRI	Gd-DTPA	(structure)	r_1=4.9mM^{-1}·s^{-1} r_2=6.3mM^{-1}·s^{-1}	Weak toxicity	Short half-life Weak signal in vivo
	Gd-EOB-DTPA	(structure)	r_1=6.9mM^{-1}·s^{-1}	High relaxivity	-
	Resovist	-	r_1=25.4mM^{-1}·s^{-1} r_2=151mM^{-1}·s^{-1}	Small dose	Poor colloidal stability
CT	Iotrolan	(structure)	-	Good colloidal solubility	Higher viscosity
	Ioversol	(structure)	-	Less side effects Good stability	Large dose
	Iohexol	(structure)	-	Good colloidal solubility Good stability	Large dose
PAI	ICG	(structure)	-	Good biocompatibility Good photoacoustic effect	Poor colloidal stability Short half-life Low cell uptake

Because the principle of T_1 imaging is based on direct interaction between the metal ions and water, the amount of metal ions of contrast agents will substantially affect their r_1 relaxivity. This leads to another disadvantage of small molecular MRI contrast agent, that is, each chelate with one paramagnetic center can only produce limited enhancement on MR signal [42]. Therefore, nanoscale Gd-based materials such as Gd_2O_3 nanoparticles [43], GdF_3 or $GdF_3:CeF_3$ nanoparticles [44, 45], and $GdPO_4$ nanoparticles [46], and Mn-based materials such as solid/hollow MnO_x nanoparticles [47, 48] and MnO_x nanosheets [49], have been extensively investigated as T_1 contrast agents. As expected, these nanoscale T_1 contrast agents exhibit higher r_1 relaxivity than their larger counterparts due to their larger surface area. For example, Park et al. synthesized lamellar structured ultrathin MnO nanoplates, which had large surface area. The r_1 value of nanoplates is 5.5 $mM^{-1}s^{-1}$, which is the highest value with reference to previously reported Mn-based MRI contrast agents [50]. In addition, it has been well-established that the surface amount of Gd^{3+} and Mn^{2+} determines the r_1 relaxivity of the resultant contrast agents. Taking advantage of high surface-to-volume ratios of nanomaterials, Gd^{3+} and Mn^{2+} have also been conjugated onto the surface of nano-carrier to develop nano contrast agents with higher r_1 relaxivity [51, 52]. Interestingly, the highly oxidized Mn is easy to be reduced in the medium reduction environment, resulting in higher magnetic moment (paramagnetic) cation species, such as Mn^{2+}, which is the basis for the design of responsive MR imaging contrast agents. Although nanoscale Gd-based materials and Mn-based contrast agents exhibit excellent prospects, there are no successful examples of their applications in RA diagnosis up to now. Therefore, it is urgent to develop functional T1 MRI contrast agents for early diagnosis of RA *via* thorough laboratory and clinical studies.

T_2 contrast agent shortens transverse relaxation time by interfering with the inhomogeneity of the external local magnetic environment. This can make the neighboring hydrogen protons to produce phase (diphase) quickly in the relaxation, and thereafter weakens the MR signal and makes the MR image darker. Iron oxide nanoparticles, such as superparamagnetic iron oxide nanoparticles (SPIONs) and ultrasmall SPIONs (USPIONs), are typical T_2 contrast agents used in clinic. Due to their high magnetic moment, SPIONs and USPIONs can accelerate the relaxation rate of hydrogen nucleus in adjacent tissues obviously [53]. The small size of SPIONs and USPIONs results in their longer blood half-life and wider biodistribution,which can better target specific tissues for *in vivo* imaging. . USPIONs exhibit a smaller hydrodynamic diameter and much less magnetic moment compared with SPIONs. SPIONs and USPIONs-enhanced T_2 MR images could be obtained by controlling T_2-weighted MR sequences. Through tuning the size of particle and length of ligand, the r_2 value of iron oxide nanoparticles can be optimized [54]. Examples from Zhang's research group confirm that SPION based contrast agents have been successfully used for RA diagnosis [37, 38]. SPIONs coated with targeting ligand and hydrophilic layer, namely, FA-glu-dex-SPION [37] and FA-PEG-b-PAA_{36}@SPION [38], are prepared for specific imaging of RA synovium lesions. After being injected into the tail vein of the antigen-induced arthritis (AIA) rats, T_2 image of RA synovium lesion is significantly darkened, indicating their good soft tissue imaging performance [37, 38].

2.2. CT imaging

CT imaging relies on the use of software programs to process X-ray images taken from different angles [55, 56], which can be used to obtain 3D images of tissues and organs of interests. Due to its high spatial resolution, high tissue penetration and high imaging speed, CT imaging has been extensively used in non-invasive cancer diagnosis to visualize morphological abnormalities [57]. The principle of CT imaging is that different tissues have different X-ray attenuation ability, which makes them present different light and shade images. Since CT imaging can differentiate the subtle internal contrast between bone and soft tissue, CT is becoming the gold standard for detecting bone damage (such as bone erosion, calcification and new bone formation) and is recommended for imaging erosion in RA and other inflammatory arthritides [58]. However, there are still some disadvantages which prevent the universal application of CT in RA diagnosis [58]. Firstly, due to the limited soft tissue contrast capabilities, CT also suffers from the same constraints as radiography. Secondly, the dosage of ionizing radiation is proportional to the size of the body part and the requirements for spatial detail. Consequently, there are only few studies on RA diagnosis using CT imaging. Therefore, it is of great significance to develop CT contrast agents for better imaging, especially for early diagnosis of RA.

CT contrast agent should be a material with good X-ray attenuation. It has been well-established that the elements with higher K-shell electron binding energy (K-edge) values within the X-ray spectrum and higher atomic numbers can substantially enhance the X-ray attenuation [59]. Typical CT contrast agents always contain elements such as iodine, gold, bismuth, ytterbium, tungsten, etc. And clinical CT contrast agents usually are derivatives of 1,3,5-triiodobenzene, such as iohexol and iopanol. Similar to small molecular MR contrast agents, small molecular CT contrast agents also suffer from high dosage, potential side effects, poor selectivity and short half-life. An effective strategy to address these issues is to conjugate iodinated compounds onto the surface of nanoparticles. Su and co-workers [60] developed a one-pot hydrothermal method to prepare iodine doped carbon quantum dots (CQDs) which can act as efficient contrast agents for CT imaging. However, considering the X-ray spectrum and its K-edge value (33 KeV), iodine is not an optimal contrast agent for CT imaging [59].

X-ray attenuation with Au should be larger than iodine, since Au has a higher atomic number than iodine. More importantly, through polymerization of iodine functionalized amphiphilic molecules or surface conjugation of iodinated molecules, nanostructured Au can package a larger amount of Au element than iodine-based nanomaterials, which can thereby lower the concentration of contrast agents [59]. Also due to its versatile surface chemistry, Au nanoparticle (AuNPs) is becoming an attractive platform for developing multi-modal imaging probes.However, the high cost of Au limits its application as contrast agents for imaging. Compared with Au, bismuth (Bi) is cheaper and has larger X-ray attenuation coefficient. The soft Bi-encapsulated polymeric nanoparticle synthesized by Lanza and co-workers [61] can offer several-fold CT signal enhancement even *in vivo*. In addition, bismuth sulfide (Bi_2S_3) is another promising Bi-based CT contrast agent [62].

2.3. Photoacoustic (PA) imaging

PA imaging is a new non-invasive and non-ionizing bioimaging technique which utilizes a pulsed laser as an energy source and ultrasonic waves as signals [63]. The principle of PA imaging is the photothermal effect. The light energy is converted to heat and the temperature of the targeted region increases, when a pulsed laser beam encounters tissues and body components such as lipid, melanin, myoglobin, and hemoglobin. This photothermal effect leads to thermo-elastic expansion which generates ultrasonic waves [64]. Due to its advantages of high penetration depth of ultrasound imaging and high spatial resolution of optical imaging, PA imaging attracts significant attentions recently [65].

To fully take advantage of PA imaging, some technical barriers such as low sensitivity and difficulty in detection of tissues blocked by air cavities or bones should be overcome[64]. An efficient strategy is to develop PA contrast agents with high photothermal coefficient. Generally, AuNPs can serve as PA imaging contrast agents, because they exhibit adjustable and excellent optical absorption properties due to the localized surface plasmon resonance (LSPR) effect [66, 67]. More importantly, the range of absorbed and scattered light can be finely tuned *via* controlling the size, morphology, and interparticle distance of AuNPs, which thereby facilitate PA imaging [68]. Since the optical absorption peak of blood is at ~520 nm, Lu and co-workers tuned the optical absorption peak of hollow gold nanospheres (AuNS) to 800 nm by controlling its size to 40~50 nm, in order to differentiate the PA signals of AuNPs and those of blood [69, 70].

PA imaging is clinically applied for visualizing synovial blood vessels by using the ultrasonic diagnostic equipment [71, 72], and demonstrates the potential for RA diagnosis. Jonathan Vonnemann et al have synthesized polysulfated gold nanorods for targeted PA imaging of inflammation in arthritis mice with high contrast [73]. Core-shell structured nanoparticles, referred to as QRu-PLGA-RES-DS NPs, which consists of quadrilateral ruthenium nanoparticles (QRuNPs) as a core and the targeted molecule dextran sulfate (DS) modified poly (lactic-co-glycolic acid) (PLGA) as a shell, have been designed and synthesized. QRu-PLGA-RES-DS NPs have been demonstrated as an excellent targeted PA imaging contrast agent for the analysis of inflammatory tissues [74].

2.4. Fluorescence (FL) imaging

In addition to MRI, CT and PA imaging, FL imaging can also provide effective diagnostic and prognostic evaluation of RA by monitoring the altered level of molecular distortion [75, 76]. Due to its advantages such as its simplicity for implementation, high sensitivity for real-time detection, and good compatibility for biomedical applications, FL imaging has been applied in pre-clinical trials for various purposes. The weak penetration ability *in vivo* is the main limitation of FL imaging. Luckily, this shortcoming can be improved by NIR FL imaging. Similar to MRI, CT and PA imaging, in order to obtain better imaging performance, the use of contrast agents is also involved in FL imaging. Organic dyes, quantum dots (QDs), carbon nanodots (C-dots), and upconversion nanoparticles (UCNPs), are extensively used FL contrast agents.

Specifically, organic dyes such as cyanines, BODIPYs, fluorescein as well as rhodamine analogues can possibly act as FL contrast agents for RA diagnosis [77, 78]. Most of these organic dyes are near-infrared (NIR) dyes, which have the advantages of good biocompatibility, high FL quantum yield, easy structure adjustment, low price and relatively high penetration due to NIR. For example, indocyanine green (ICG) whose emission peak and quantum yield of ICG are 835 nm and 13%, can be used in angiography and approved by FDA for clinical use.

Semiconductor QDs, which consist of elements from Groups II-VI, II-V, III-V, IV-VI, I-VI, I-III-VI, IV [79], exhibit good potential as FL contrast agents, because of their long FL lifetime, high quantum yield, narrow emission band, large Stokes shift, and possible NIR emission to achieve deeper imaging [80]. It has been well-established that emission wavelength of semiconductor QDs can be tuned by changing elemental composition and particle size of QDs [79]. For example, elemental composition of QDs can be finely tuned by controlling the core precursor ratios, and thereby red-shifting the emission wavelength of the as-prepared QDs [81]. Similarly, the size of QDs can be finely tuned by varying the synthesis temperature, and thereby its emission wavelength is changed [82].

UCNPs which is an important category of FL contrast agent, can absorb NIR light and emit FL with a shorter wavelength [83, 84]. UCNPs have good photostability and low background noise. UCNPs are consisted of matrix material, activator and sensitizer [85]. The rare earth elements such as Er^{3+}, Tm^{3+}, Ho^{3+}, Eu^{3+}, generally used as activators which largely determine the emitting light of UCNPs. For example, Er^{3+} doped UCNPs emit green light [86], while Tm^{3+} and Ho^{3+} doped UCNPs emit blue [87] and red light [88], respectively.

Recently, carbon dots (C-dots) is becoming an important member of FL contrast agents due to its advantages such as chemical inertness, excellent biocompatibility, tunable emission spectra, broad excitation spectra and high photostability [89, 90]. Similar to semiconductor QDs, the emission wavelength of C-dots can also be finely tuned by altering the precursors and varying the synthetic methods [91]. For example, the emission light of C-dots can be tuned from blue to red *via* surface oxidation and/or element doping which can be achieved by the addition of passivators such as reagents rich in amino group during the synthesis [92]. In addition, the size of C-dots can be tuned by varying the synthetic methods, which can also affect its emission property. Generally, the larger the size, the longer the emission wavelength.

With the development of FL technology and its contrast agent, FL is possible to be used as a diagnostic tool for RA. It can provide images with high sensitivity for diagnosis and pathogenesis of RA. For example, a FL turn-on probe is developed by Huang Feng and co-workers to detect hypochlorite biomarkers at the RA site for RA diagnosis [93]. The specific C=N bond cleavage reaction triggered by HOCl at RA site will initiate the FL "OFF-ON" response of the probe. Although FL imaging has a bring future, its application in in RA diagnosis is still at early stage.

2.5. Multimodal imaging

Although there are a lot of molecular imaging technologies which provide great help for clinical diagnosis, their application in RA diagnosis is limited due to the inherent defects of their respective imaging principles. For example, FL imaging has poor tissue penetration, although it has the advantages of simplicity for implementation, high sensitivity for real-time detection, and good compatibility for biomedical applications [94]. In contrast, MRI has high spatial contrast resolution of soft tissues, which can

clearly show synovial lesions, bone edema, cartilage destruction in early RA patients [37, 38], but it suffers from the low sensitivity to osteosclerosis and bone erosion [95, 96]. Therefore, single imaging technology is difficult to provide comprehensive and accurate information for RA diagnosis. Multimodality imaging might provide a new way to solve this problem.

Multi-modality imaging refers to the combination of more than two imaging methods, so that it has multiple imaging functions at the same time to achieve the effect of complementary advantages, thereby improving the accuracy of diagnostic results. The key of multimodal imaging lies in the fusion of multiple imaging contrast agents. Kim [97] et al developed a nanocomposite for targeted T_2-MR and NIR optical imaging of inflamed paws of CIA mice (**Fig. 4A**). In this design, arginine-glycine-aspartic acid (RGD) is the active targeting molecule towards RA site, while Fe and Au function as the contrast agent for T_2-MR imaging and NIR optical imaging respectively. In the absence of the Nd-Fe-B magnet of 2.3 T, increased absorbance intensity was observed in the inflamed paws of CIA mice after being injected with the nanocomposite, and absorbance intensity slowly decreased over time (**Fig. 4B**). Similar results were observed in T_2-MR imaging, indicating targeted delivery and effective accumulation of the nanocomposite in the inflamed paws of CIA mice (**Fig. 4C**). The combination of optical imaging and MRI can overcome the weak penetration of optical imaging and the low sensitivity of MRI, so as to achieve better diagnostic effect for RA. In addition to MR/NIR imaging, multi-modal imaging such as FL/PA [98], FL/MR [99], and US/PA [100] have also been successfully applied for RA diagnosis.
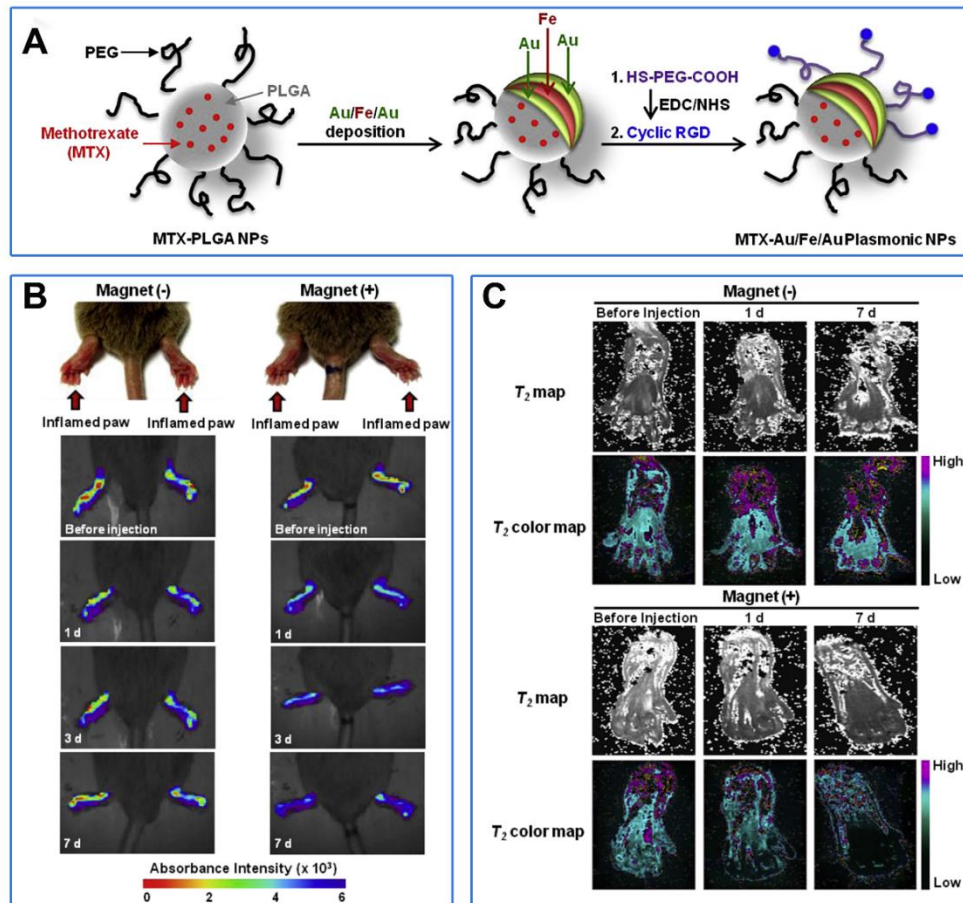
Fig. 4. (A) The preparation of MTX-Au/Fe/Au plasmonic NPs. (B) In vivo NIR absorbance images and (C) in vivo T_2 MR images of inflamed paws of CIA mice injected intravenously with Au/Fe/Au plasmonic NPs and caged with (+) or without (-) a magnet. Copied with permission [97]. Copyright 2015, Elsevier Ltd.

2.6. Stimuli-responsive imaging

The contrast agents can effectively improve the imaging quality, but they also circulate in the body. This results in their accumulation not only in the RA site, but also in other parts of the body with a certain retention rate. This means that not only the signals from lesion sites but also those from healthy sites will be enhanced, which lower the signal-to-background ratio and thereafter the sensitivity of imaging. Very recently, research focus is shifting from "always on" probe to "turn on" probe, that is, stimuli-responsive imaging.

The microenvironment of RA is similar to that of tumor, which is rich in reactive oxygen species, acidic condition and redox environment. These factors can be used as targets for responsive imaging. For example, inflammatory response-related HOCl can be used as RA biomarkers. Based on the principle of specific HOCl-triggered C=N bond cleavage reaction, two FL turn-on probes have been designed and demonstrated for stimuli-responsive imaging of RA *in vivo* with substantially improved sensitivity [93]. In another example, ROS is used as RA biomarkers. Based on the mechanism of luminescent resonance energy transfer (LRET), UCNPs were conjugated with rhodamine-B-labeled HA to prepare stimuli-responsive probe, HAR-UCNPs (**Fig. 5A**) [101]. In this design, UCNPs serve as the energy donor to excite the luminescence of rhodamine B *via* LRET process. The ROS can specifically cleave HA to release rhodamine B and stop LRET process, resulting in the luminescence changing from rhodamine B to UCNPs (**Fig. 5B**). *In vitro* and *in vivo* experiments confirm that the HAR-UCNPs is highly responsive to ROS with high sensitivity (**Fig. 5C & 5D**). And the upconversion luminescence

(UCL) signals from CIA mice was significantly stronger than those from healthy mice and MTX-treated CIA mice (**Fig. 5D** & **5E**). Obviously, due to the low imaging background and substantially improved signal-to-noise ratio, the sensitivity of stimuli-responsive imaging is much higher than that of target imaging, holding the promise for future early diagnosis of RA.
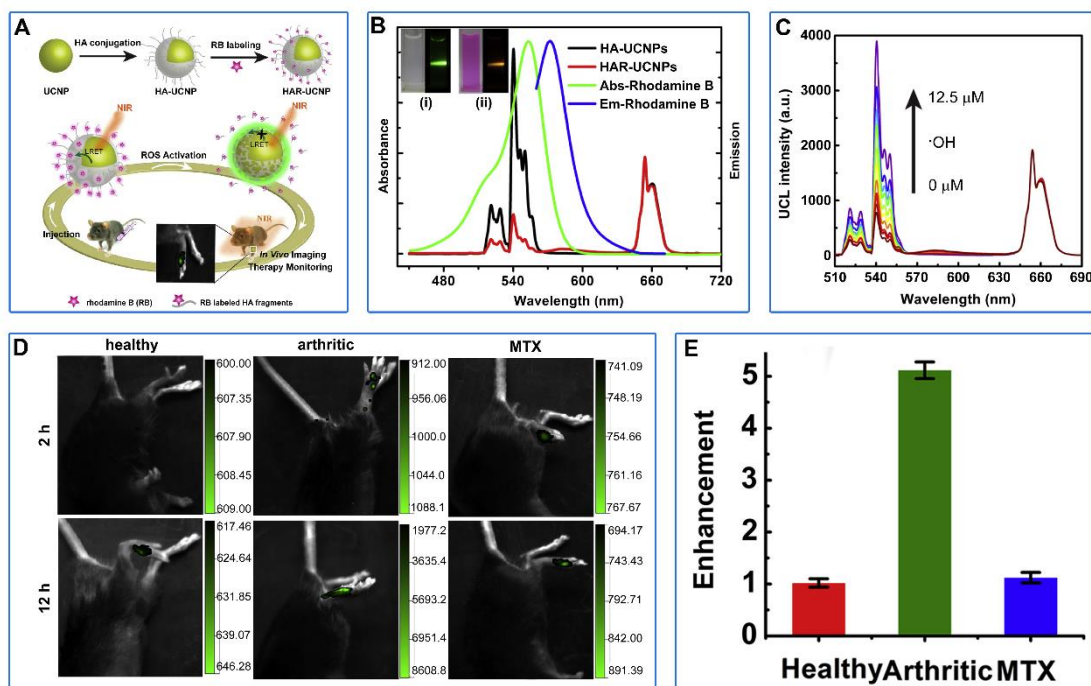
Fig. 5. (A) Schematic illustration of HAR–UCNP. (B) UV–vis absorption and emission spectra of rhodamine B, UCL spectra of HA–UCNPs and HAR–UCNPs. The illustrations show HA-UCNP (i) and HAR-UCNP (ii) under daylight (left) and 980nm laser irradiation (right), respectively. (C)UCL spectra of HAR–UCNPs upon gradual addition of •OH. (D) In vivo UCL images of healthy mice, arthritic mice, and MTX-treated mice after local injection of HAR-UCNPs. (E) The enhancement of UCL in the arthritic joint in 12 h compared to 2 h post-injection for treatment monitoring. Copied with permission [101]. Copyright 2015, Elsevier Ltd.

Up to now, there are few studies on stimuli-responsive imaging of RA. However, since the microenvironment of RA is similar to that of tumor, lessons can be learned from the responsive imaging of tumor sites. For example, the principle of magnetic exchange coupling effect (MECE) has been employed to design GSH-responsive MR probes for tumor imaging [102]. MECE means that when the distance L between two magnetic nanoparticles is less than the critical distance D, with the decrease of the distance between them, the interface exchange coupling effect decreases, the total susceptibility of the system decreases, and the image changes are caused. When L>D, MECE gradually disappeared, and the magnetic susceptibility of the system remained unchanged. The probe was composed of Fe_3O_4 and $CoFe_2O_4$, and was connected by disulfide bond in the middle to form Fe_3O_4-S-S-COFe_2O_4$.When GSH exists, disulfide bond is cut off, the distance is greater than D, the susceptibility decreases and SWI image darkens (**Fig. 6A**). When the Fe_3O_4-S-S-CoFe_2O_4$ injected to a tumor bearing mice, the brightness of SWI and T_2 images on the tumor site immediately dimmed, while the relative signal intensity of SWI images changed more than that of T_2 images, and the relative signal changes of SWI increased with time, reaching the peak at 1 h, about 85% (5 times of T_2), and lasted for 2 h (**Fig. 6A**). The probe responds to GSH, which greatly improves the sensitivity. The imaging sensitivity could be further improved by increasing signal-to-noise ratio and using SWI sequence.

Y. S. Chen [103] et al designed a PA probe responsive to external light stimulation. The probe is composed of poly(n-isopropylacrylamide) (PNIPAM) with volume change photothermal stimulus response and gold nanorods as a PA contrast agent. When the probe is concentrated in the tumor site through EPR effect and irradiated by near-infrared light, it generates heat energy, PNIPAM decreases in size and reduces the particle size of nanoparticles, which rapidly diffuses the generated thermal energy to the surrounding medium and improves the PA signal (**Fig. 6B**). The dynamic contrast-enhanced PA image highlights the suppression of background signals from blood vessels, PA enhancement was shown only in tumor areas where nanostructures clustered before and after continuous wave laser stimulation. The design of this probe and the use of dynamic PA imaging can effectively reduce the influence of background signals such as blood vessels, so as to improve the imaging quality of tumors and achieve better diagnostic results.

Based on CBT condensation reaction, Wang et al [104] designed and synthesized a CT imaging probe with dual stimulus response of pH/GSH. The probe is a small molecular probe composed of iodized benzene ring, citraconic motif and cysteine. When it reached tumor tissue, acidic conditions induced release of citraconic motif and GSH trended to cut off the disulfide bond of cysteine to produce active monomers. The cyano group of CBT and 1, 2-aminothiol of Cys would generate amphiphilic dimers through CBT condensation reaction, and formed amphiphilic dimers that self-assembled to form nanoparticles that stay in the cell longer and improved imaging quality (**Fig. 6C**). When the functional probes were injected intravenously into the tumor bearing mice, the CT signal of the injection probe group was significantly increased, the highest ΔHu was 21, and it could stay in the tumor site for a longer time; while in the control probe group, the highest ΔHu was only 15.91, and there was no significant tumor signal

(**Fig. 6C**). This indicated that the functional probe could react responsibly in the tumor site and self-assembled to form nanoparticles with larger size, thus prolonging the residence time in the tumor site and improving the diagnostic effect.

Bouche et al [105] reported a hydrogel nanoparticle loaded with AuNPs as CT and PA imaging contrast agents. Among them, the polyphosphazene polymers of nanogels can be selectively degraded by ROS, thereby releasing AuNPs and reducing PA signal. Therefore, this probe can be used for PA/CT ratiometric ROS imaging (**Fig. 6D**). *In vitro* inflammatory cell experiment, LPS-induced RAW264.7 produced inflammatory cells. When co-incubated with nanoparticles, PA signal significantly decreased, while CT signal remained unchanged. When nanoparticles were co-incubated with normal cells, both PA and CT signals remained unchanged (**Fig. 6D**). This probe provides responsive imaging of inflammatory cells, and RA is also an inflammatory disease, which may provide some inspiration for us to design a probe for RA. PA/CT dual mode can combine the high sensitivity of optical imaging and the deep tissue imaging of CT imaging to carry out more accurate imaging of the lesion site and achieve better diagnostic results.

Guo [106] et al designed a trypsin responsive NIR FL/MR imaging dual-imaging composite nanoparticle/polypeptide coacervate nanoprobes. The probe is composed of polyacrylate modified Fe_3O_4 magnetic nanoparticles and Cy5.5 modified poly-L-lysine for MRI and trypsin reaction substrate /NIRF, respectively. The fluorescence of Cy5.5 is quenched due to dye aggregation effect. These two substances are self-assembled to form the nanoprobe. When it enters the tumor with overexpression of trypsin, the poly-L-lysine in the probe reacts with the enzyme to lyse the probe and release Cy5.5, so restore the fluorescence. At the same time, due to the smaller particle size, the uptake of particles by the cells is increased, thus improving the signal of MR imaging. After intravenous injection of nanoparticles to tumor bearing mice, the FL/MR signal of trypsin overexpression tumor group was significantly increased, but there was no significant difference in the non-trypsin expression tumor group, indicating that the probe has the potential of pancreatin responsive FL / MR imaging.
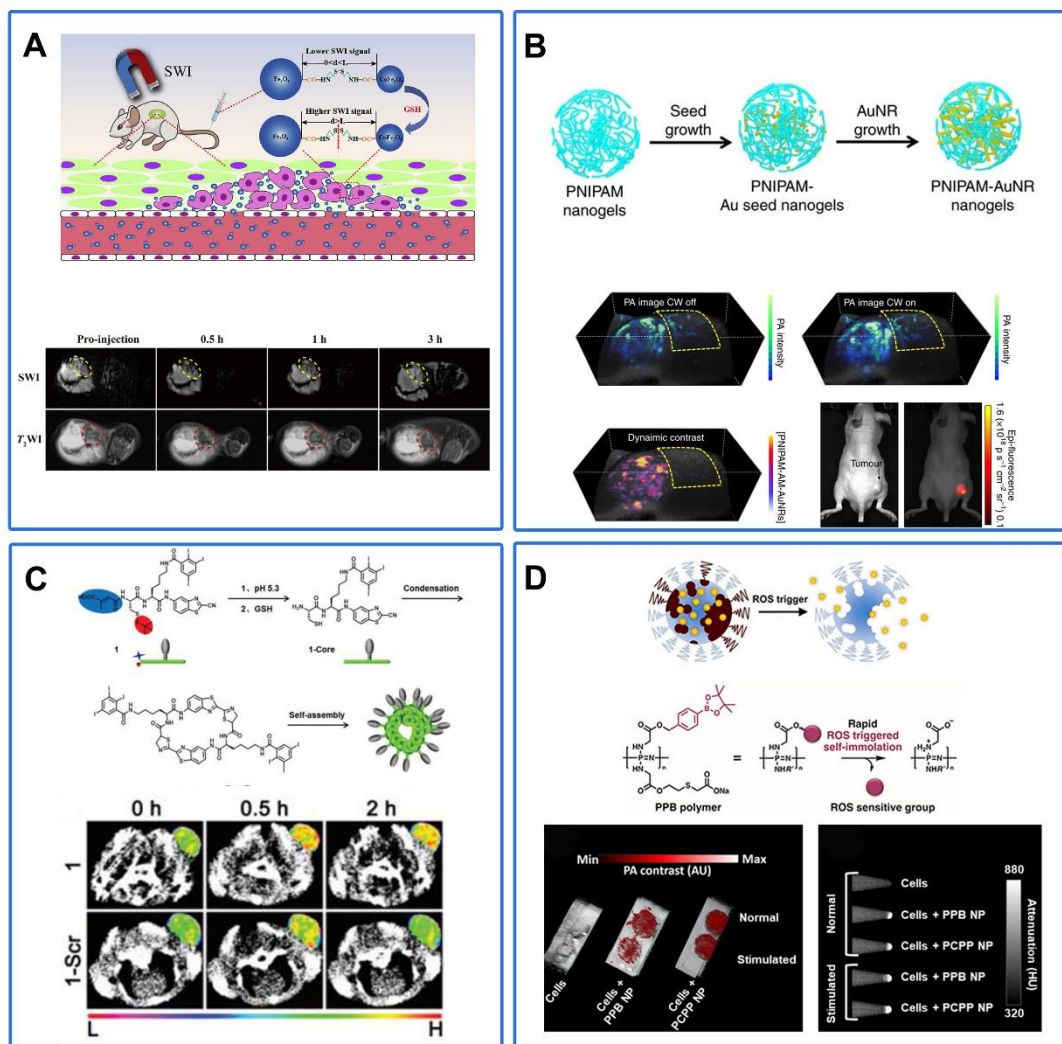
Fig. 6. (A) Schematic illustration of GSH responsive MR imaging probe Fe_3O_4-S-S-COFe$_2$O$_4$ and imaging effect. Copied with permission [102]. Copyright, 2020 Elsevier Ltd. (B) Schematic illustration of NIR responsive PA imaging probe PNIPAM and imaging effect. Copied with permission [103]. Copyright 2017, Springer Nature. (C) Schematic illustration of GSH/pH responsive CT imaging probes and imaging effect. Copied with permission [104]. Copyright 2018, The Royal Society of Chemistry. (D) Schematic illustration of ROS responsive PA/CT imaging probes and imaging effect. Copied with permission [105]. Copyright 2019, American Chemical Society.

3   Nanotherapy for RA

Although conventional RA treatment has made considerable progress with certain therapeutic effect, it is still compelling to develop advanced therapies to overcome the risks of dose escalation-induced defunctionalization and therapeutic tolerance. Among all the advanced therapies, nanotherapy is a rising technology that gives an innovative therapeutic platform to treat RA with minimal side effects and lower costs [107]. The nanoscale size in combination with the flexibility for surface functionalization of the nanocarriers, enables target delivery of therapeutic agents in lesion sites *via* passive or active targeting [8, 108]. Target delivery can significantly reduce the damage of off-target distribution to other organs. In addition, nanocarriers can protect therapeutic agents from rapid biodegradation, resulting in sustained drug release and extended cyclic kinetics. More importantly, the bioavailability and solubility of specific drugs can be significantly improved by nanocarriers, since they can transport drugs by neglecting their intrinsic bioavailability and solubility [109-113]. All of those properties of nanotherapy can significantly decrease the dose of therapeutic agents and protect patients from invasion to the affected areas [114]. Nanocarriers including nanocapsules, dendrimers, liposomes, micelles and nanogels, have been extensively used for target delivery of anti-rheumatoid drug. In this section, recent advances in the application of nanotherapy for RA treatment will be discussed in detail.

3.1. Chemotherapy

With the deepening of research on nanotherapy, anti-RA drug-loaded nanocarriers have been developed for RA chemotherapy to optimize the therapeutic efficacy and safety profile. **Table 3** summarizes some representative nanocarriers which have been used for specific delivery of therapeutic agents with passive or active targeting strategies. Taking advantages of nanocarriers, therapeutic agents can be targetedly delivered to the inflammatory sites and be controllably released for a sustained period of time.

As the most widely used nanocarriers, liposomes which encapsulate dexamethasone (Dex) as anti-RA drug, have been successfully used for RA treatment [115]. To optimize *in vivo* half-life and inflammatory joint targeting capacity, liposomes with a diameter of 100 nm are synthesized and surface functionalized with slightly negative charged 10% 5 kDa PEG. Pharmacodynamic studies performed in a CIA mouse clearly demonstrate that the anti-arthritic efficacy of Dex is significantly improved after being encapsulated in liposomes.

Table 3
Some typical therapeutic drug delivery strategies for RA.

Drug/Agent	Carrier System	Animal model	Delivery strategy	Ref.
Anti-TNF	NP based on albumin	Phase II clinical trial	Macrophages	[116]
Betamethasone	PLGA NP	AA rats and AbIA mice	Inflamed joint	[117]
Collagen	PLGA NP	CIA mice	Lymphocytes	[118, 119]
Curcumin	Nanomicelle	CIA rats	Cytokines/VEGF	[120]
Dexamethasone	Liposome/ Micelle/HPMA copolymer	AA rats		[121]
Dexamethasone	PCL-PEG micelle	AA rats	ELVIS	[122]
Dex-g-MTX	Micelle	CIA mice	Macrophages	[123]
Etanercept	SPL nanocomplex	CIA rats	EPR	[124]
Fe-bLf	Chitosan-CP-Fe-bLf-NC	CIA mice	Macrophages	[125]
Fumagillin	PFC NP	Inflammatory arthritis mice	αvβ3 integrin	[126]
Fumagillin	PFOB NP	AIA mice	αvβ3 integrin	[127]
Glucocorticoids	PEG liposome	CIA mice	Inflamed synovial lining	[128]
IL-1ra c-DNA	Chitosan NP	AIA rats/CIA mice	EPR/Macrophages	[129, 130]
Indomethacin	Micelle	AA rats	EPR	[131]
Methotrexate	DSNP	CIA mice	SR-A	[132]
Methotrexate	MFC-MSN	AIA mice	Macrophages	[133]
Methotrexate	HSA	CIA mice	Macrophages	[99]
Methotrexate	PAMAM Dendrimers-G5-FA	CIA rats	EPR/Folate receptor	[134]
Methotrexate	PLGA/Au NP	CIA mice	αvβ3-Integrin	[135]
Neutrophil membrane	PLGA	CIA mice	Pro-arthritogenic factors	[136]
Notch1	Poly-siRNA-tGC	CIA mice	Macrophages	[137]
Prednisolone	PEG-liposome	AIA rats	EPR/Macrophages	[138]
Prednisolone	pH-sensitive polymeric micelle	CIA mice	Macrophages	[139]
siRNA against TNF	tGC	CIA mice	Macrophages	[140]
siRNA against TNF, IL-1, IL-6, IL-18	Lipoplexes	CIA mice	Macrophages	[8, 141]
SOD	Liposome	AA rats		[142]
Tocilizumab	HA-AuNP	CIA mice	VEGF/IL-6 receptor	[143]
γ-secretase inhibitor	HA-NP	CIA mice	Macrophages	[144]

To further improve targeting efficiency, active targeting is extensively employed for nanocarriers by conjugation with a targeting moiety such as peptides, antibodies, carbohydrates, oligonucleotides, etc. For example, it was found that the acidic and cysteine-rich protein (SPARC) was overexpressed in the synovium and synovial fluid of RA patients. Therefore, taking advantages of the intrinsic high affinity of SPARC for albumin, MTX was loaded into human serum albumin nanomedicines (referred to as MTX@HSA NMs) for

RA therapy (**Fig. 7A & 7B**) [99]. *In vivo* therapeutic evaluations suggested higher accumulation and longer retention of MTX@HSA NMs in inflammatory joints (**Fig. 7C**). In comparison with free MTX, the progression of RA in CIA mice was attenuated with better efficacy by the MTX@HSA NMs with even a half MTX dosage (**Fig. 7D & 7E**). The lower MTX dosage, the fewer side effects. This biomimetic drug delivery systems validated the high efficacy of active targeting for RA therapy.
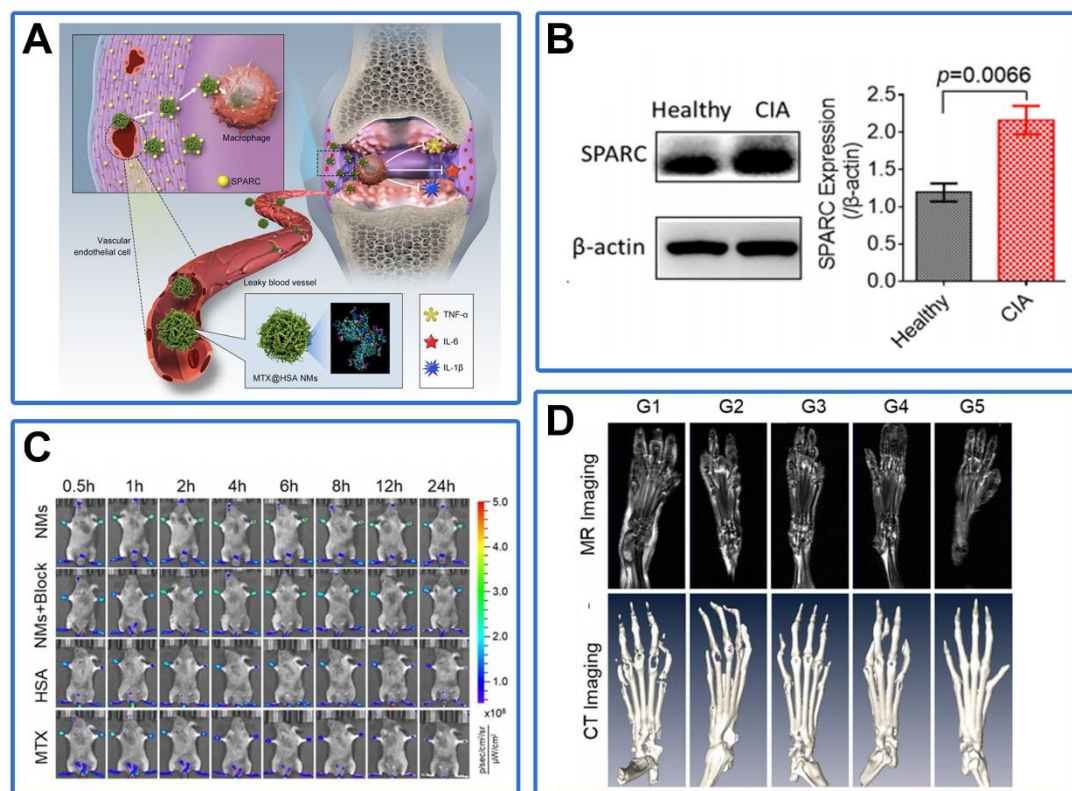
Fig. 7. (A) Methotrexate-loaded human serum albumin nanomedicines (MTX@HSA NMs) for the treatment of rheumatoid arthritis by biomimetic delivery. (B) Western blotting (WB) assay of SPARC expression in healthy and CIA mice. (C) In vivo fluorescence images of CIA mice from the different treatment groups. (D) Magnetic resonance imaging (MRI) and micro computed tomography (CT) imaging of the feet of mice in the different treatment groups. (G1: PBS, G2: MTX-2.5 mg/kg, G3: MTX-5.0 mg/kg, G4: MTX@HSA NMs-2.5 mg/kg, G5: MTX@HSA NMs-5 mg/kg). Copied with permission [99]. Copyright 2019, American Chemical Society.

In the study of Shi and co-workers, tumor necrosis factor-related apoptosis-inducing ligand (TRAIL) was employed as inflammation-targeting ligands for targeting the activated M1 macrophages in the inflammatory sites of RA [98]. Through genetic bioengineering, TRAIL was expressed onto the umbilical vein endothelial cell (UVEC) membrane, and thereafter TRAIL-UVECs membrane was coated onto hydroxychloro- quine (HCQ) loaded PLGA nanoparticle for RA management using the broad-spectrum anti-inflammatory strategy.According to the design, these nanoparticles could specifically deliver HCQ to the inflammatory joints and neutralize the secreted cytokines, thus alleviating RA progression.

The combination therapy which uses more than one therapeutic agent for RA treatment has been strongly recommended by various clinical studies. It has been proven that single drug dose can be decreased and drug resistance can be avoided by using the combination therapy [145]. For example, in a randomized trial, the combination of MTX and ETA exhibits better therapeutic effect in RA patients with severe symptoms [145]. However, most of current nanocarriers still deliver single drug. Therefore, future studies in RA nanotherapy should focus on incorporation of multiple drugs into a single nanocarrier for improving therapeutic effects and decreasing side effects.

3.2. Biotherapy

Since RA disrupts patients' immune balance, pro-inflammatory cytokines such as TNF-α, TGF-β, IL-1 and IL-6 are activated and recruited in the pathological process of RA. Therefore, the inhibitors for pro-inflammatory cytokines, including TNF-α inhibitors (INF, ETA, adalimumab (ADA)), the T-cell co-stimulation inhibitor abatacept, the IL-6 receptor inhibitor TCZ, and new antibodies (rituximab, certolizumab pegol, golimumab) which target the B-cell-specific CD 20 antigen, have been used for RA therapy in clinic [146]. These biological agents have also been extensively investigated for enhancing their therapeutic effects by conjugating onto the surface of nanoparticles. For example, TCZ was modified onto the surface of hyaluronate-gold nanoparticle (referred to as HA-AuNP/TCZ) for RA treatment [143]. *In vivo* experiments revealed that the best therapeutic effect was observed on CIA rats treated with HA-AuNP/TCZ, as evidenced by the suppression of inflammatory cells infiltration and the restoration of bone erosion. As expected, the typical markers of the macrophage lineage such as IL-6 and CD68 was found to be down-regulated upon treatment with HA-AuNP/TCZ.

In another example, TNF-α antibody, a targeting moiety for inflammatory sites, is conjugated onto the surface of nanomicelles which are synthesized by simply mixing negatively charged amphiphilic polyelectrolyte and positively charged ETA, TNF-α antibody [124]. *In vitro* experiments demonstrated that bioactivity of ETA in nanomicelles was substantially improved under physiological conditions and

its plasma concentration could be maintained for an extended period of time. More importantly, *in vivo* experiments demonstrated that, in comparison with control group, lower paw thickness, decreased level of TNF-α, and better histopathological status were observed for CIA mice treated with nanomicelles.

Gene therapy is also being tested for RA treatment. For example, siRNA targeting TNF-α was polymerized with thiolated gycol chitosan (TGC) polymers to synthesize a nanocomplex for RA treatment [140]. As expected, the nanocomplex was accumulated at the arthritic joint sites in CIA mice, and exhibited TNF-α gene silencing efficacy.

3.3. Photothermal therapy (PTT)

In recent years, phototherapy which includes PTT and photodynamic therapy (PDT), has attracted ever-growing attention not only in biomedical research but also in clinical practice, due to its relative non-invasive and gentle treatment [147]. During PTT, photo-sensitizers are used to convert light especially NIR light into heat to destroy disease tissues due to hyperthermia. **Table 4** summarizes the photosensitizers frequently used for phototherapy. In the combination with target delivery of photosensitizers, precisely controlled release of heat can be achieved in a dose and time-dependent manner. There is no doubt that PTT can induce cell death around inflammatory tissues, but the temperature should be precisely controlled to avoid unnecessary tissue damage during light exposure.

Table 4
Summary of photosensitizers used for phototherapy.

Classification	Nano-carrier	Drug-loaded	Application	Ref.
Ce6	Chitosan	-	PDT	[148]
Copper	$Cu_{7.2}S_4$	-	PTT, PDT	[149]
	Au	Infliximab/certolizumab	Optoacoustic	[150]
	Au-DEN	MTX	PTT, PDT	[151]
Gold	Au/Fe/Au	MTX	PTT	[97]
	Au/PLGA	MTX	PTT	[135]
	Polysulfated gold	-	Optoacoustic tomography	[73]
ICG	PLGA/PFP/OI	-	PSDT	[152]
Iron	Fe_3O_4	-	PTT	[153]
	BPD-MA	-	PDT	[154]
Porphyrins and its derivate	PEG^{5k}-Cys_4-Por_4-CA_4	-	PTT, PDT	[155]
	Porphyrins	-	PDT	[156]
	$TSPP/TiO_2$	-	PDT	[157]
	$TSPP/TiO_2$	-	PDT	[158]
Talaporfin sodium	Talaporfin sodium	-	PDT	[159]
$TPCC_4$	Chitosan	-	PDT	[148]
$TPPS_4$	Chitosan	-	PDT	[148]
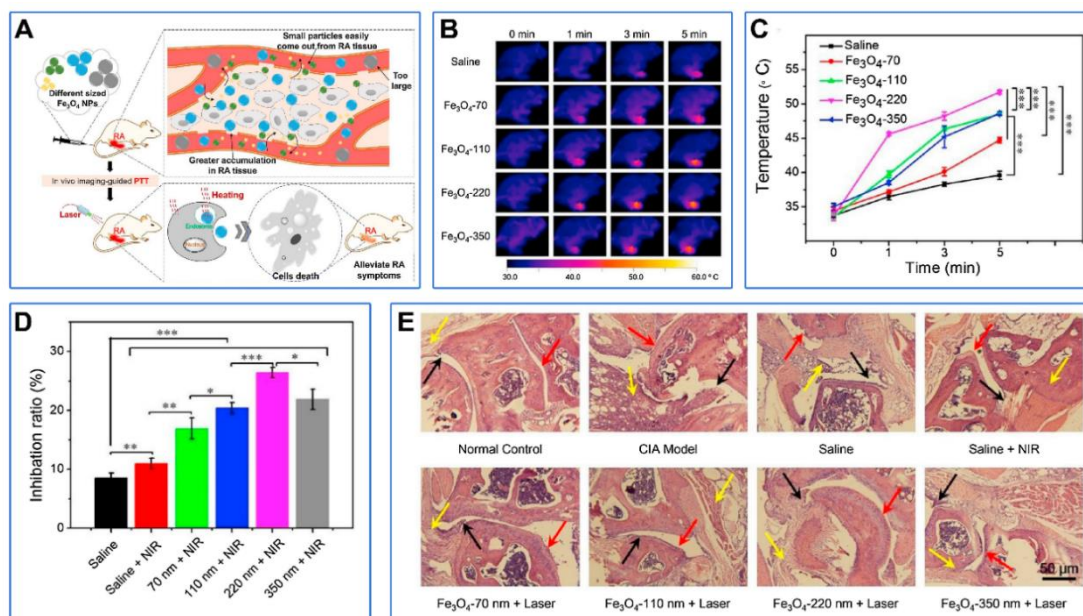
Fig. 8. (A) Schematic depiction of the optimal size of Fe_3O_4 NPs for RA photothermal therapy. (B) Thermal imaging of CIA mice treated with PTT therapy at different times after intravenous injection of saline or Fe3O4 nanoparticles for 24 h. (C) The average temperature of the paw region of mice under different irradiation time. (D) The RA inhibition ratio post treatment. (E) Micrographs of H&E stained joint tissues of CIA mice in different groups. Copied with permission [153]. Copyright 2018, Elsevier B.V.

Since gold nanoparticles (AuNPs) exhibit high photothermal conversion efficiency and anti-inflammatory effect, they have been successfully employed as nanomedical platform for RA treatment. For example, IR780, a bioactive NIR activator, is encapsulated into gold-core nanovesicles for RA treatment. Due to the synergistic effect between AuNPs and IR780, the photothermal conversion efficiency is significantly enhanced, where temperature can go up to 42 ± 2 °C in 3 mins and last for at least 10 mins [151].

Since magnetic iron oxide (Fe_3O_4) nanoparticles also has a higher photothermal conversion efficiency under irradiation of NIR light, it has been used for ablating activated inflammatory cells in RA therapy. Zhang and co-workers found that the size of Fe_3O_4 nanoparticles has a great influence on its therapeutic effect, due to the increase of vascular leakage pore size in RA (**Fig. 8A**) [153]. In their study, Fe_3O_4 nanoparticles with a diameter of 220 nm induced the strongest photothermal effect, which was evidenced by the raised high temperature at 51.7 °C of inflamed paw 51.7 °C (**Fig. 8B, 8C**) and better inflammatory inhibition effect in RA therapy (**Fig. 8D**). Furthermore, a remarkable decrease in inflammatory cell infiltration, cartilage damage, and synovial hyperplasia could be observed in the histopathological images (**Fig. 8E**).

3.4. Photodynamic therapy (PDT)

Similar to PTT, photosensitizers are also needed in PDT for the production of ROS under irradiation of light with a specific wavelength [160]. ROS produced *in situ* can destroy the disease tissues with no invasion and low adverse effects. PDT also holds great promise for RA treatment, since cytotoxic effects can be induced in synovial membrane after photosensitizers are specifically accumulated in the inflammatory sites and activated by corresponding light [161]. However, the challenge of PDT application in RA treatment still exists in the insufficient oxygen caused by hypoxic microenvironment of the RA site and oxygen consumption during PDT.

As a commercially available photosensitizer for PDT, the potential of talaporfin sodium for synovectomy in CIA rats has been examined. On the day of PDT treatment, extensive cell necrosis was only observed in the inflammatory synovium of CIA rats. After 56 days of treatment, bone and cartilage erosion was inhibited [159]. Benzoporphyrin derivative monoacid ring-A (BPD-MA) is the second-generation photosensitizer, which has also been explored for RA treatment. Results confirmed that BPD-MA mediated PDT was specific to pathologic tissues, as evidenced by that synovial necrosis was only observed in the inflammatory sites while no damage was detected in surrounding normal tissues [154]. Similar to BPD-MA, another extensively used photosensitizers in PDT, porphyrins and its derivate, was only detected in the inflammatory sites of RA rabbits, rendering a new approach for RA diagnosis [156].

3.5. Synergy of multiple therapeutic approaches

As demonstrated above, chemotherapy, PTT and PDT, all demonstrate the great potential for effective RA treatment *in vivo*. The combination of phototherapy and chemotherapy can obtain the synergistic effect and greatly optimize the treatment effect of RA. Nanomaterials provide a robust framework to realize this vision.
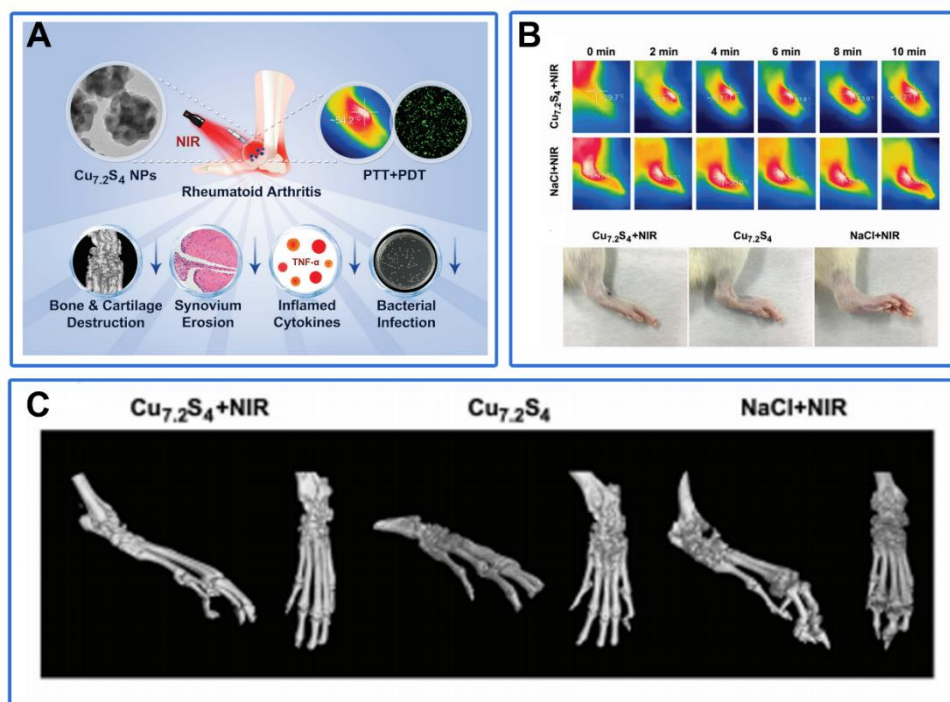
Fig. 9. (A) Schematic illustration of the $Cu_{7.2}S_4$ NPs combined with PTT and PDT therapy for the RA treatment. (B) Thermal imaging and photos of paws of the CIA rats in different treatment groups after 28 d. (C) Micro-CT imaging of paws of different groups in vivo [149]. Copyright 2018, WILEY-VCH Verlag GmbH & Co. KGaA, Weinheim.

As a first-line drug for RA, MTX is conjugated onto the surface of nanoparticles which can serve as photosensitizers, for a combination of PTT and chemotherapy. In a typical example, AuNPs were functionalized with RGD as the targeting moiety and MTX as the therapeutic agent [135]. Upon irradiation, AuNPs convert light energy into heat, resulting in the increased temperatures and thereafter the release of MTX into the inflamed paws of CIA mice. Higher therapeutic efficacy and lower dose-dependent adverse effect were observed for CIA mice treated with this AuNPs-based nanomedicine than those treated with MTX only. MTX has also been conjugated onto the surface of Au/Fe/Au plasmonic nanoparticles not only for a combination of PTT and chemotherapy but also enhanced targeting by magnet [97]. The enhanced retention in inflammatory region and the combination of PTT, results in high therapeutic efficacy and low dose-dependent side effect.

Under irradiation, copper-based nanomaterial can not only convert light into heat, but also produce ROS. Therefore, they can simultaneously serve as the photosensitizer for PDT and PTT. In addition, Cu is beneficial for chondrogensis and otseogensis. Therefore, copper-based nanomaterial, for example, $Cu_{7.2}S_4$ nanoparticles have been successfully applied for the treatment of CIA rats to alleviate RA using both PDT and PTT (**Fig. 9A**) [149]. Under NIR irradiation, the temperature raised by 27°C (from 27°C to 54°C) in 10 min in the presence of $Cu_{7.2}S_4$ nanoparticles, while only raised by 5°C (from 27°C to 32°C) in the absence of $Cu_{7.2}S_4$ nanoparticles (**Fig. 9B**). Most importantly, after being treated with $Cu_{7.2}S_4$ nanoparticles, the paws of CIA rats turned into normal ones, showing the lowest clinical indexes while having higher bone volume/total volume and bone mineral density (BMD) (**Fig. 9C**). In addition, $Cu_{7.2}S_4$ nanoparticles exhibited strong antibacterial capability and thus preventing bone from bacterial infection.

The combination of PDT and sonodynamic therapy (PSDT) for RA treatment has also been realized by using the PLGA nanoparticles loaded with ICG [152]. Cytotoxic effects on synoviocytes mediated by PSDT were confirmed by more evident cell apoptosis and more serious cell damage than control group. In addition, upon treated with PSDT, more intracellular ROS was generated in MH7A cells. This was the first attempt to treat RA by PSDT for better penetrability on the lesion.

3.6. Stimuli-responsive and biomimetic nanoparticles for RA treatment

The stimuli-responsive nanoplatforms which can target specific inflammatory mediators and thereafter efficiently suppress the pathologic inflammation cascade, is capable of alleviating symptoms of RA and subsequent joint destruction. Drug leakage can be substantially avoided since stimuli-responsive nanoplatforms can only be triggered to release drug at lesion sites [162]. Therefore, significantly decreased toxicity and substantially enhanced treatment efficacy can be realized by using stimuli-responsive nanoplatforms [163].
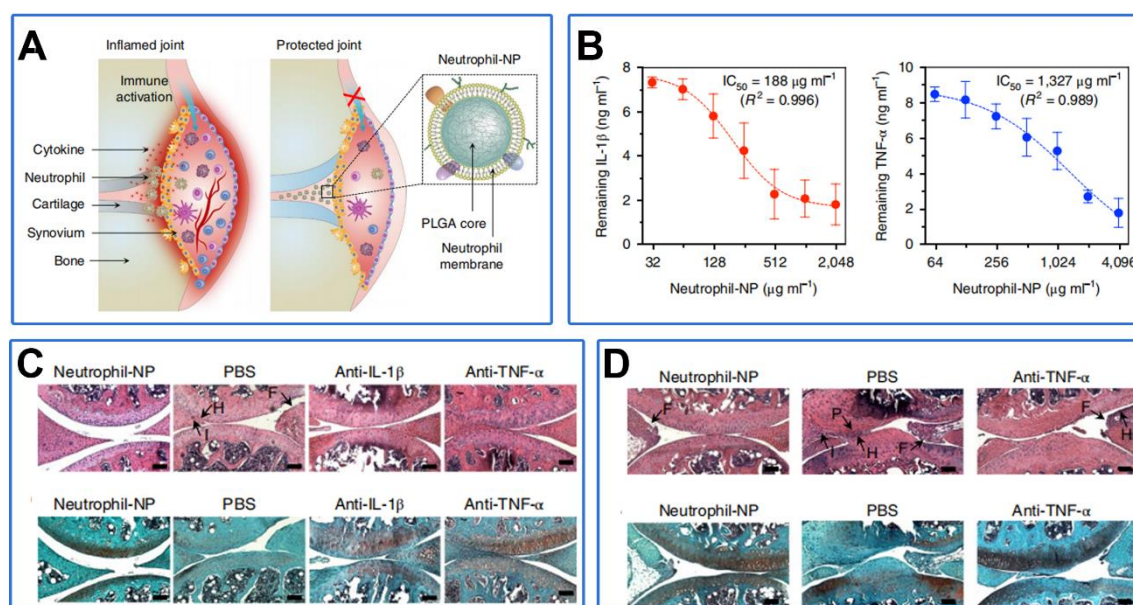
Fig. 10. (A) Schematic illustration of neutrophil-NPs for suppressing synovial inflammation and ameliorating joint destruction in RA. (B) Binding capacity of neutrophil-NPs with IL-1β (left) and TNF-α (right). (C&D) Micrographs of H&E stained (top) and safranin-O stained (bottom) knee sections from (C) CIA mouse, (D) human TNF-α transgenic mouse of inflammatory arthritis in different treatment group. Copied with permission [136]. Copyright 2018, Springer Nature.

In addition, the biomimetic nanoparticles have also gained increased research attentions due to their excellent biocompatibility and good targeting capacity. Since RA regions and tumors exhibit many similarities such as hypoxia and leaky vasculature, design principles of nanocarriers for cancer can be adapted for RA. For example, Zhang et al. fused neutrophil membrane to polymeric cores to synthesize biomimetic nanoparticles for RA treatment (**Fig. 10A**) [136]. As designed, by presenting strong binding capacity towards IL-1β and TNF-α, these biomimetic nanoparticles could target deep matrix of the cartilage, neutralize proinflammatory cytokines, and suppress synovial inflammation (**Fig. 10B**). As a result, a substantial therapeutic efficiency was observed in CIA mouse and human transgenic arthritic mouse (**Fig. 10C & 10D**).

4   Integration of diagnosis and treatment for RA

Theranostics which perfectly integrate diagnosis and treatment, have attracted increasing research attentions in the past decade [164]. Compared with single diagnosis or treatment method, it has obvious advantages in personalized medical treatment, real-time monitoring treatment process and feedback of the treatment effect. The carrier is the basis of the integration of functions of diagnosis and treatment. A good carrier design should enable a better combination of diagnosis and treatment. Nanomaterials with the characteristics of fine size, morphology and surface chemistry, can be used as an excellent carrier to make it easy to combine two or more components. Therefore, nanomaterials have become one of the most valuable and important tools to develop multifunctional theranostic probes with high signal strength, good targeting effect and controllable metabolic dynamics. In this section, we will introduce several typical nano-carriers for the theranostics, and discuss the possibility of their application in the simultaneous diagnosis and treatment of RA.

4.1. Liposome

Liposomes which consist of an aqueous core surrounded by one or more phosphor-lipid bilayer membranes, are spherical particles with diameter in the range of 25 to 1000 nm [165]. Since phospholipid molecules have both hydrophilic groups and hydrophobic groups, liposomes are capable of entrapping both hydrophilic and hydrophobic drugs. There are three different ways to integrate therapeutic and imaging materials into liposomes. Firstly, hydrophobic materials can be embedded/adjusted in lipid bilayer [166]. Secondly, hydrophilic nanoparticles can be encapsulated into an inner aqueous compartment of liposome [167]. Finally, different nanoparticles can be adsorbed over the liposome surface based on their physical and chemical properties [168]. Due to the non-toxic, flexible, biocompatible and completely biodegradable properties, liposomes have been extensively investigated for not only effective drug delivery but also the theranostics [169]. However, the disadvantage of liposomes as carriers is that they can be easily removed from the blood by the lymphatic and reticuloendothelial systems.

Gan and co-workers reported a typical example of liposome-based theranostics [170]. In this liposome system, the drug MTX is loaded in the inner aqueous compartment, the fluorescent imaging contrast agent is embedded in the lipid caliper, and the target molecule iRGD is grafted externally at the outer layer. The liposome can split and release the drug under the action of ultrasound to realize controlled release. As designed, *in vivo* FL imaging experiment confirmed that liposomes are accumulated in RA joints by showing significantly stronger fluorescence. More importantly, the diagnostic imaging and therapeutic benefit were simultaneously achieved by using this liposome combined with ultrasound imaging.

4.2. Gold nanoparticles (AuNPs)

AuNPs can be synthesized through wet chemistry methods, and their shape and size can be well controlled to meet specific needs. Typically, the size of AuNP ranges from 10 nm to 200 nm, and its morphology can be tailored, resulting in isotropic (spherical, triangular, octahedral, and tetrahedral) or asymmetric shape (Rod, wire, star) [171]. Besides the morphology, the surface AuNP can be easily modified, leading to the biomolecule conjugations with the enhanced biocompatibility. The versatile chemistry of AuNPs makes the conjugation of therapeutic and/or contrast agents onto AuNPs easier. In the recent decade, AuNPs have been widely adopted in many biomedical engineering studies such as optical biosensing platform, targeted drug delivery carrier and imaging contrasting agent for diagnostics[172].

Thanks to the special optical and electronic properties, AuNPs are explored as contrasting agents for different diagnostic imaging methods such as PA imaging [69, 70], CT imaging [59] and photothermal imaging [135]. AuNPs mediated radiotherapy and PTT are also developed based on the special properties of AuNPs [151]. On the other hand, since surface modification allows targeted biomolecules or antibody binding, AuNPs-mediated diagnosis and immunization methods have good specificity. Therefore, AuNPs have become potential nanocarriers of theranostic platform for RA treatment.
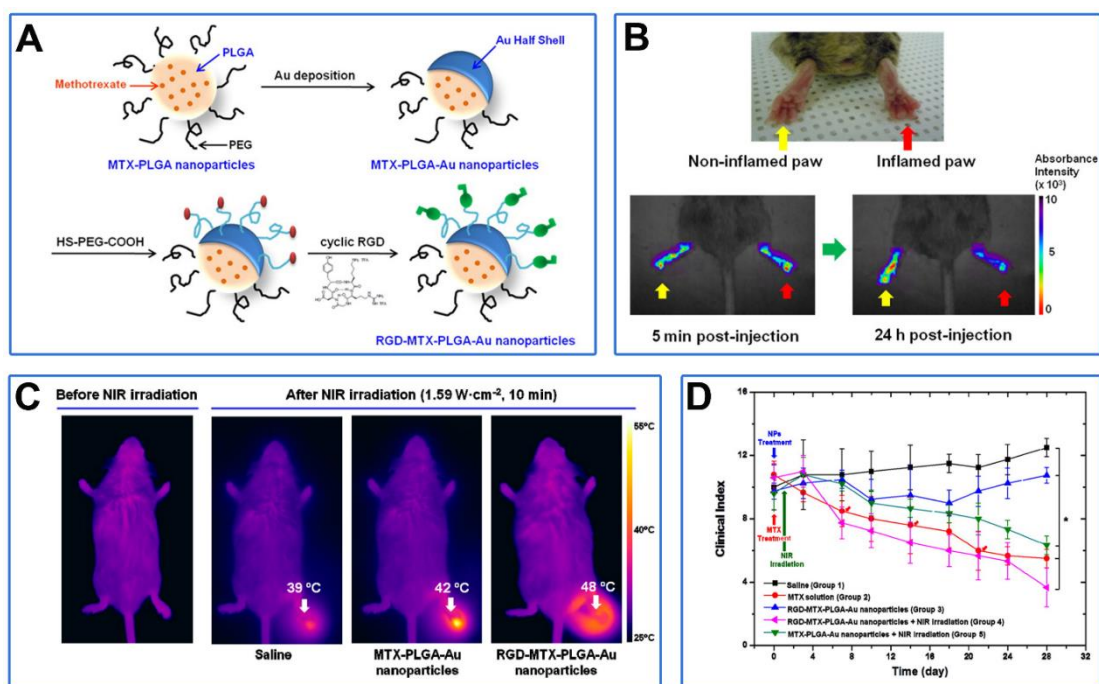
Fig. 11. (A) Schematic illustration of RGD-MTX-PLGA-Au nanoparticles. (B) In vivo NIR absorbance images of paws in CIA mouse injected intravenously with RGD-MTX-PLGA-Au nanoparticles. (C) Thermal images of inflamed paw in CIA mice after different treatment before and after NIR exposure. (D)Clinical index versus time for CIA mice in different treatment group. Copied with permission [135]. Copyright 2012, American Chemical Society.

For example, a nanotheranostic platform for RA treatment was prepared by encapsulating AuNPs and MTX into the pegylated-poly (DL-lactic-co-glycolic acid) nanosphere [173]. In this nanotheranostic platform, AuNPs served dual functions of PA imaging and PTT therapeutic agents, while MTX is a first-line drug for RA chemo-therapy. Therefore, the diagnostic PA imaging and therapeutic benefits from the synergy of PTT/chemotherapy were simultaneously demonstrated.

In another example of nanotheranostic platform (referred to as RGD-MTX-PLGA-Au nanoparticles) for RA treatment, MTX was encapsulated into PLGA nanosphere which was thereafter deposited with half Au shell and conjugated with RGD (**Fig. 11A**) [135]. In this nanotheranostic platform, MTX served dual functions of NIR absorbance imaging and chemotherapy, while Au shell served as PTT therapeutic agents. Compared to non-inflammatory paws, a significant color change can be observed in the inflammatory paw of *in vivo* NIR absorbance images, suggesting the specific accumulation of RGD-MTX-PLGA-Au nanoparticles in RA sites (**Fig. 11B**). The temperature of the irradiated paw increased to 48 °C for the mice treated with RGD-MTX-PLGA-Au nanoparticles, substantially higher than control groups (**Fig. 11C**). More importantly, the clinical index of group 4 is the lowest among the five groups, indicating that the synergy of PTT/chemotherapy has the best therapeutic effect (**Fig. 11D**).

4.3. Polymeric nanoparticles

There are two main kinds of polymeric nanoparticles for nanomedicine applications. The polymeric nanoparticles can be formed by abruptly aggregated block copolymers of different hydrophobicity into core-shell micelles in an aqueous environment [174]. Dendrimer which is made from synthetic or natural elements such as nucleotides, sugars, and amino acids, is another kind of polymeric nanoparticles [175]. Through covalent or hydrogen bond, and/or hydrophobic interaction, not only small molecule drugs but also macromolecular drugs such as proteins and nucleic acid, can be conjugated onto the surface of or encapsulated into the core of polymeric nanoparticles [176]. Besides therapeutic agents, targeting moiety and diagnostic agents can also be conjugated onto the surface of or encapsulated into the core of polymeric nanoparticles. In addition, ligands of polymeric nanoparticles such as HA, folic acid (FA), dextran, mannose, tuftsin, and etc., allows for specific binding to certain receptors on the surface of activated macrophages, leading to receptor-mediated endocytosis. Compared with liposomes, slower drug release is observed and less frequent administration is required [177].
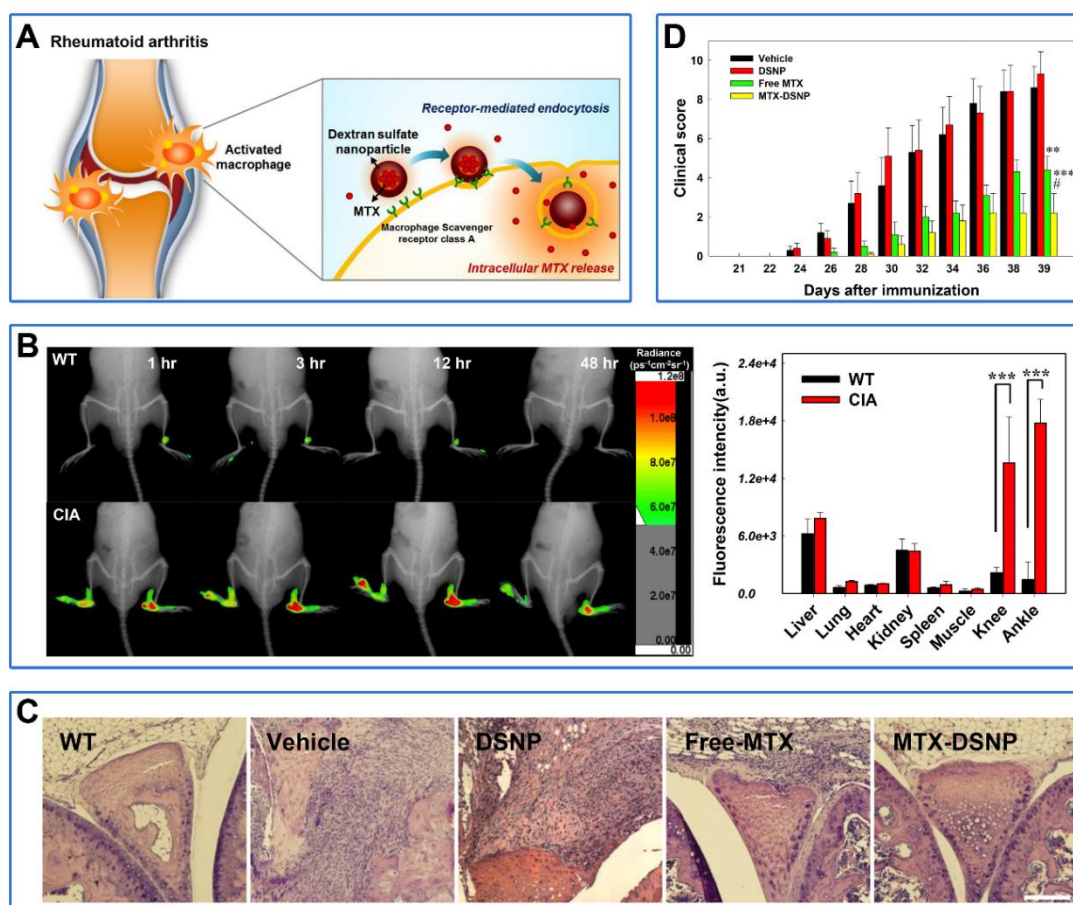
Fig. 12. (A) Schematic illustration of DSNPs as nanocarriers for targeted RA therapy. (B) Biodistribution of FPR-675-labeled DSNPs in WT and CIA mice. (C) Micrographs of H&E stained knee joints of mice. (D) Clinical score versus time for CIA mice in different treatment group. Copied with permission [132]. Copyright 2017, Elsevier Ltd.

It has been reported that there is overexpressed macrophage scavenger receptor class A (SR-A) on the surface of activated macrophages which can specifically bind to dextran sulfat (DS) [178]. Therefore, 5β-cholanic acid was conjugated to a DS backbone to prepare an amphiphilic polysaccharide which could self-assemble into nanoparticles (referred to as DSNPs). The DSNPs were further loaded with MTX for chemotherapy and labeled with FPR-675 for FL imaging (**Fig. 12 A**) [132]. *In vitro* experiments confirmed that DSNPs could effectively enter into activated macrophages *via* SR-A mediated endocytosis. *In vivo* experiments revealed that DSNPs accumulated in the inflammatory paws of CIA mice by exhibiting strong FL signal, while no FL signal was observed in wild type (WT) mice (**Fig. 12 B**). H&E staining (**Fig. 12 C**) and clinical evaluation (**Fig. 12 D**) revealed that DSNPs could effectively alleviate RA symptoms, validating DSNPs as a useful theranostic platform for RA.

4.4. SPION

SPIONs consist of iron oxide as core and a biocompatible and hydrophilic polymer as shell to improve their water solubility, stability and biocompatibility [179]. The SPION agents ferucarbotran (60 nm) and ferumoxide (120-180 nm) have been approved by FDA for clinical use as MR contrast agents. Through surface functionalization, SPIONs can be conjugated with targeting ligands, other imaging contrast agents and therapeutic agents to serve as non-invasive theranostic tools for RA [180]. For example, a SPION-based theranostic platform was developed by co-encapsulating MTX as the therapeutic agent and SPIONs as the MR contrast agents into PLGA nanoparticles [181]. In addition, anti-CD64 antibody was functionalized onto the surface of nanoparticles for specific targeting activated macrophages. This theranostic platform has been successfully demonstrated for simultaneous diagnosis and treatment of RA.

4.5. Carbon nanodots (CDs)

Based on the advantages of CDs, it is considered as a promising candidate for building multifunctional theranostic platforms. At present, most of the theranostics platforms based on CDs take cancer as the research model, but there is no report on RA. However, because of the similarity between the microenvironment of RA and tumor, it has great reference significance. Sun [182] et al synthesized a red emission CDs (RCDs) rich in amino groups, and then grafted the photosensitizer chlorin e6 (Ce6) onto the surface of the RCDs s through amide bond. Ce6 in Ce6-RCDs has PA imaging and PDT treatment functions, while RCDs have FL/PT/PTT functions. When Ce6-RCDs was injected intravenously, it gathered in tumor tissue through EPR effect and performed FL/PA/PT tri-modal imaging to achieve more accurate diagnostic results. At the same time, PDT/PTT combined therapy can achieve better tumor inhibition effect.

Using manganese phthalocyanine as precursor, Jia [183] et al synthesized FL/MR dual-modal imaging CDs by hydrothermal method, and then self-assembled with DSPE-PEG to form nanoparticles. The nanoparticles can also produce singlet oxygen to enhance the therapeutic effect of PDT. After entering the body, the nanoparticles reach the tumor site through EPR effect. The overexpression of H_2O_2 in the tumor site catalyzes the decomposition of MnO_2 into Mn^{2+} and produces oxygen, which enhances PDT treatment and restores the MR signal.

Jia [184] et al synthesized hypocrella bambusae CDs (HBCDs) by one-step hydrothermal method using hypocrella bambusae as precursor. Hypocrella bambusae has photodynamic antiviral and anticancer activities, while CDs has FL/PA and PTT effects. HBCDs can accumulate at tumor sites through EPR effect, and can be used as FL/PA-guided PDT/PTT therapy, and has good theranostic functions for cancer.

In summary, CDs have a good prospect in the construction of integrated theranostic systems, because they have FL/PA imaging function, and some CDs also have PDT/PTT function. Moreover, CDs can be doped with heterogeneous elements in a simple way to obtain new functions.

5   Conclusion

RA is an autoimmune musculoskeletal disorder that has caused severe disability in patients and has an enormous impact on the lives of people worldwide [185]. Therefore, the effective diagnosis and treatment of RA is of great significance to alleviate patients' pain and improve the cure rate. In this review, we summarize the current common treatment strategies and imaging technologies, explore the possibility of their application in RA, analyze several nanocarriers and discuss their potential as integrated probes for RA diagnosis and treatment.

Firstly, a variety of commonly used medical imaging technologies are summarized in this review, including FL, MRI, PA and CT imaging. These imaging techniques have been used in the diagnosis of RA with certain effects. Besides, common contrast agents for these imaging techniques are also listed, including their advantages and disadvantages, in order to provide more options for researchers. Then, we describe the multimodal imaging of RA. Multimodal imaging refers to the combination of various imaging technologies to make up for their shortcomings, so as to obtain high-quality imaging images. However, "always on" probes will not only accumulate in the RA site, but will also be retained to some extent in other parts of the body, resulting in high background signals. Therefore, stimuli-responsive imaging was introduced. It refers to that only when the focus is reached, the imaging signal is generated from zero, so as to obtain the image with a high signal-to-noise ratio.

Secondly, several common treatment strategies are summarized including chemotherapy, biotherapy, PTT and PDT. The commonly used drugs such as MTX, AuNPs and porphyrins are listed and discussed. The application of these therapies in RA are also summarized and their effectiveness on therapy is discussed. Furthermore, the synergy of multiple therapeutic approaches is comprehensively discussed. Compared with single therapy, combined therapy has better therapeutic effects and is expected to improve the therapeutic efficacy of RA. At last, the application of stimuli-responsive therapy of RA is also evaluated, which can significantly improve the treatment effect and reduce the drug dosage with good application prospect.

Finally, the integration of diagnosis and treatment based on several common nanocarriers including liposomes and AuNPs, is summarized. The possibility of their applications in the integration of diagnosis and treatment is also discussed. These carriers have been widely used in the theranostic of tumor with unique advantages. Moreover, the methods of loading contrast agents and drugs with these carriers and their applications in theranostics of RA are also discussed. At last, stimuli-responsive theranostics are also discussed, which are emerging as one of the trends of diagnosis and treatment of RA in the future.

At present, theranostic nanoprobes integrated with diagnosis and treatment are developing rapidly. They are not only used in tumors, Alzheimer's disease, but also in RA. However, due to the strong self-background of the contrast agent and the difficulty of nanodrug delivery, the development of the probe for RA is limited. Therefore, stimuli-responsive theranostic attracts researchers' attention. Stimuli-responsive theranostics with imaging and drug release responding to specific disease site, is of high significance for improving imaging quality, enhancing treatment effect and reducing toxic and side effects. The local microenvironment of RA has unique characteristics

including high ROS level and low pH, which can be used to trigger responsive signals, thereby improving the diagnosis and treatment effects of RA. There are few studies on the stimuli-responsive theranostic of RA so far. However, since the microenvironment of RA is similar to that of tumor, lessons can be learned from the responsive theranostics of tumors. Definitely, stimuli-responsive theranostics of RA will be one of the most promising research topics in the future.

Table 5

Abbreviations in Table 2, Table 3 and Table 4.

Abbreviation	Definition	Abbreviation	Definition
AA	Adjuvant-induced arthritis	PAI	Photoacoustic imaging
ABIA	Anti-type II collagen antibody induced arthritis	PAMAM	Poly (amidoamine)
AIA	Antigen-induced arthritis	PCL	Poly(ε-caprolactone)
BPD-MA	Benzoporphyrin derivative monoacid ring-A	PEG	Polyethylene glycol
Chitosan-CP-Fe-bLf-NC	Chitosan coated calcium phosphate encapsulating iron saturated bovine lactoferrin nanocarrier	PFC	Perfluorocarbon
CA	Cholic acid	PFOB	Perfluorooctylbromide
Ce6	Chlorin e6	PFP	Perfluoro-n-pentane
CIA	Collagen-induced arthritis	PLGA	Poly(D,L-lactic/glycolic)
CT	Computed tomography	Por	Dendritic oligomers of pyropheophorbide-a
DEN	Dendron	PSDT	Photodynamic therapy followed by sonodynamic therapy
DSNP	Dextran sulfate nanoparticle	QY	Quantum yield
ELVIS	Extravasation through leaky vasculature and subsequent inflammatory cell-mediated sequestration	r_1	Longitudinal relaxation rate
Em	Fluorescence emission peak	r_2	Transverse relaxation rate
EPR	Enhanced permeability and retention	Ref.	Reference
FITC	Fluorescein Isothiocyanate	Resovist	Superparamagnetic iron oxide nanoparticles coated with carboxy dextran
FLI	Fluorescence imaging	RGD	Arginine-glycineaspartic acid
Gd-EOB-DTPA	gadolinium ethoxybenzyl diethylenetriaminepentaacetic acid	SOD	Superoxide dismutase
Gd-DTPA	Gadolinium-diethylenetriaminepentaacetic acid	SPL	Temperature sensitive amphiphilic polyelectrolyte
HPMA	N-(2-hydroxypropyl) methacrylamide	SR-A	Macrophage scavenger receptor class A
HSA	Human serum albumin	tGC	Thiolated glycol chitosan
ICG	Indocyanine green	TNF	Tumor necrosis factor
MFC-MSN	manganese ferrite and ceria NP-anchored mesoporous silica NP	TPCC4	Tetra-phenyl-chlorin-tetra-carboxylate
MRI	Magnetic resonance imaging	TPPS4	Tetra-phenyl-porphyrin-tetra-sulfonate
OI	Oxygen and indocyanine green	TSPP	Tetera suplhonatophenyl porphyrin

Notes

The authors declare no competing financial interest.

Acknowledgment(s)

References

[1] G.S. Firestein, Nature 423 (2003) 356-361.

[2] S. Dolati, S. Sadreddini, D. Rostamzadeh, et al., Biomedicine & Pharmacotherapy 80 (2016) 30-41.

[3] Q. Guo, Y.X. Wang, D. Xu, et al., Bone Research 6 (2018) 15-19.

[4] T. Sokka, B. Abelson, T. Pincus, Clin Exp Rheumatol 26 (2008) S35-61.

[5] J.M. Davis, E.L. Matteson, Mayo Clin Proc 87 (2012) 659-673.

[6] A.K. Shrivastava, A. Pandey, J Physiol Biochem 69 (2013) 335-347.

[7] J. Hwang, K. Rodgers, J.C. Oliver, et al., Int J Nanomed 3 (2008) 359-371.

[8] C.T.N. Pham, Wires Nanomed Nanobi 3 (2011) 607-619.

[9] S.M.J. Paulissen, J.P. van Hamburg, W. Dankers, et al., Cytokine 74 (2015) 43-53.

[10] K. Roy, R.K. Kanwar, J.R. Kanwar, Int J Nanomed 10 (2015) 5407-5420.

[11] L. Danks, H. Takayanagi, J Biochem 154 (2013) 29-39.

[12] F.C. Arnett, S.M. Edworthy, D.A. Bloch, et al., Arthritis Rheum 31 (1988) 315-24.

[13] D. Aletaha, T. Neogi, A.J. Silman, et al., Arthritis Rheum 62 (2010) 2569-81.

[14] V. Majithia, S.A. Geraci, Am J Med 120 (2007) 936-939.

[15] H. Visser, Best Pract Res Cl Rh 19 (2005) 55-72.

[16] A. Chinese Rheumatology, Zhonghua nei ke za zhi 57 (2018) 242-251.

[17] F.M. McQueen, Best Pract Res Cl Rh 27 (2013) 499-522.

[18] A. Barile, F. Arrigoni, F. Bruno, et al., Radiol Clin N Am 55 (2017) 997-1007.

[19] L. Jans, I. De Kock, N. Herregods, et al., Annals of the Rheumatic Diseases 77 (2018) 958-959.

[20] C.H. Lee, W. Srikhum, A.J. Burghardt, et al., Int J Rheum Dis 18 (2015) 628-639.

[21] L.M.H. da Mota, B.A. Cruz, C.V. Breno, et al., Rev Bras Reumatol 51 (2011) 199-219.

[22] M.A. D'Agostino, L. Terslev, P. Aegerter, et al., RMD Open 3 (2017) e000428.

[23] A.N. Colebatch, C.J. Edwards, M. Ostergaard, et al., Annals of the Rheumatic Diseases 72 (2013) 804-814.

[24] C. Gaujoux-Viala, L. Gossec, A. Cantagrel, et al., Joint Bone Spine 81 (2014) 287-297.

[25] B. Hodkinson, E. Van Duuren, C. Pettipher, et al., South African medical journal = Suid-Afrikaanse tydskrif vir geneeskunde 103 (2013) 576-585.

[26] M. Ostergaard, C. Peterfy, P. Conaghan, et al., J Rheumatol 30 (2003) 1385-1386.

[27] S. Umar, M. Asif, M. Sajad, et al., Int. J. Drug Dev. & Res. 4 (2012) 210-219.

[28] S. Mitragotri, J.W. Yoo, Archives of Pharmacal Research 34 (2011) 1887-1897.

[29] S.S. Wang, J. Lv, S.S. Meng, et al., Advanced Healthcare Materials 9 (2020).

[30] G.T. Hermanson, Bioconjugate techniques. 2nd edition. ed., San Diego, 2008.

[31] H.M. Chen, W.Z. Zhang, G.Z. Zhu, et al., Nat Rev Mater 2 (2017).

[32] M.E. Caldorera-Moore, W.B. Liechty, N.A. Peppas, Accounts Chem Res 44 (2011) 1061-1070.

[33] Z. Yang, J.B. Song, W. Tang, et al., Theranostics 9 (2019) 526-536.

[34] X.Y. Wong, A. Sena-Torralba, R. Alvarez-Diduk, et al., Acs Nano 14 (2020) 2585-2627.

[35] H. Wang, X. Chen, Expert Opin Drug Del 6 (2009) 745-768.

[36] Y.M. Cai, T.M. He, K.X. Wang, Physics Bulletin (2006) 1-5.

[37] F. Dai, M. Du, Y. Liu, et al., J Mater Chem B 2 (2014) 2240-2247.

[38] Y. Zhong, F. Dai, H. Deng, et al., J Mater Chem B 2 (2014) 2938-2946.

[39] Y.N. Fang, L.F. Zhou, J.K. Zhao, et al., Carbon 166 (2020) 265-272.

[40] Y. Pan, J. Yang, Y.N. Fang, et al., J Mater Chem B 5 (2017) 92-101.

[41] Z. Hou, Q. Wang, Z. Guo, et al., J Drug Target 28 (2020) 398-407.

[42] X. Qian, X. Han, L. Yu, et al., Adv Funct Mater 30 (2020).

[43] J.Y. Park, M.J. Baek, E.S. Choi, et al., Acs Nano 3 (2009) 3663-3669.

[44] F. Evanics, P.R. Diamente, F.C.J.M. van Veggel, et al., Chemistry of Materials 18 (2006) 2499-2505.

[45] E.N.M. Cheung, R.D.A. Alvares, W. Oakden, et al., Chemistry of Materials 22 (2010) 4728-4739.

[46] H. Hifumi, S. Yamaoka, A. Tanimoto, et al., J Am Chem Soc 128 (2006) 15090-15091.

[47] H.B. Na, J.H. Lee, K. An, et al., Angew Chem Int Ed Engl 46 (2007) 5397-5401.

[48] T. Kim, E.J. Cho, Y. Chae, et al., Angew Chem Int Ed Engl 50 (2011) 10589-10593.

[49] H.H. Fan, Z.L. Zhao, G.B. Yan, et al., Angew Chem Int Edit 54 (2015) 4801-4805.

[50] M. Park, N. Lee, S.H. Choi, et al., Chemistry of Materials 23 (2011) 3318-3324.

[51] Y. Pan, W.D. Chen, J. Yang, et al., Anal Chem 90 (2018) 1992-2000.

[52] Y.P. Shi, Y. Pan, J. Zhong, et al., Carbon 93 (2015) 742-750.

[53] N. Lee, H. Kim, S.H. Choi, et al., Proc Natl Acad Sci U S A 108 (2011) 2662-2667.

[54] Z. Li, P.W. Yi, Q. Sun, et al., Adv Funct Mater 22 (2012) 2387-2393.

[55] M. Shilo, T. Reuveni, M. Motiei, et al., Nanomedicine (Lond) 7 (2012) 257-269.

[56] N. Lee, S.H. Choi, T. Hyeon, Adv Mater 25 (2013) 2641-2660.

[57] T. Hussain, Q.T. Nguyen, Adv Drug Deliv Rev 66 (2014) 90-100.

[58] M. Ostergaard, M. Boesen, Radiol Med 124 (2019) 1128-1141.

[59] Y. Liu, K. Ai, L. Lu, Acc Chem Res 45 (2012) 1817-1827.

[60] H. Su, Y. Liao, F. Wu, et al., Colloids Surf B Biointerfaces 170 (2018) 194-200.

[61] D. Pan, T.A. Williams, A. Senpan, et al., J Am Chem Soc 131 (2009) 15522-15527.

[62] Y.X. Xiong, F. Sun, P. Liu, et al., Chemical Engineering Journal 378 (2019).

[63] L. Nie, X. Chen, Chem Soc Rev 43 (2014) 7132-7170.

[64] X. Li, J. Kim, J. Yoon, et al., Adv Mater 29 (2017).

[65] K. Sato, R. Shintate, M. Fujiwara, et al., Jpn J Appl Phys 58 (2019).

[66] Y.S. Chen, W. Frey, S. Kim, et al., Nano Lett 11 (2011) 348-354.

[67] H. Moon, D. Kumar, H. Kim, et al., Acs Nano 9 (2015) 2711-2719.

[68] Q. Fu, R. Zhu, J. Song, et al., Adv Mater 31 (2019) e1805875.

[69] W. Lu, Q. Huang, G. Ku, et al., Biomaterials 31 (2010) 2617-2626.

[70] P.K. Jain, K.S. Lee, I.H. El-Sayed, et al., J Phys Chem B 110 (2006) 7238-7248.

[71] C. Kim, T.N. Erpelding, L. Jankovic, et al., Biomed Opt Express 1 (2010) 278-284.

[72] S. Mallidi, G.P. Luke, S. Emelianov, Trends Biotechnol 29 (2011) 213-221.

[73] J. Vonnemann, N. Beziere, C. Bottcher, et al., Theranostics 4 (2014) 629-641.

[74] X. Chen, X. Zhu, L. Ma, et al., Nanoscale 11 (2019) 18209-18223.

[75] D. Golovko, R. Meier, E. Rummeny, et al., Int J Clin Rheumtol 6 (2011) 67-75.

[76] V.S. Schafer, W. Hartung, P. Hoffstetter, et al., Arthritis Res Ther 15 (2013) R124.

[77] Y. Pu, D. Wang, J. Qian, et al., Materials China 36 (2017) 103-111.

[78] X.C. Wang, G. Chang, R.J. Cao, et al., Prog Chem 27 (2015) 794-805.

[79] K.J. McHugh, L.H. Jing, A.M. Behrens, et al., Advanced Materials 30 (2018).

[80] D. Kim, N. Lee, Y.I. Park, et al., Bioconjug Chem 28 (2017) 115-123.

[81] H.S. Choi, Y. Kim, J.C. Park, et al., Rsc Adv 5 (2015) 43449-43455.

[82] E. Cassette, T. Pons, C. Bouet, et al., Chemistry of Materials 22 (2010) 6117-6124.

[83] T.P. Mokoena, E.C. Linganiso, V. Kumar, et al., J Colloid Interf Sci 496 (2017) 87-99.

[84] S. Babu, J.H. Cho, J.M. Dowding, et al., Chem Commun 46 (2010) 6915-6917.

[85] E. Hong, L.M. Liu, L.M. Bai, et al., Mat Sci Eng C-Mater 105 (2019).

[86] C. Renero-Lecuna, R. Martin-Rodriguez, R. Valiente, et al., Chemistry of Materials 23 (2011) 3442-3448.

[87] F. Vetrone, V. Mahalingam, J.A. Capobianco, Chemistry of Materials 21 (2009) 1847-1851.

[88] W. Liu, J.S. Sun, X.P. Li, et al., Opt Mater 35 (2013) 1487-1492.

[89] H.X. Li, X. Yan, D.S. Kong, et al., Nanoscale Horiz 5 (2020) 218-234.

[90] C.Q. Yi, Y. Pan, Y. N. Fang, Environmental, et al., Novel Nanomaterials for Biomedical, Energy and Environmental Applications (2019) 137-188.

[91] M. Zheng, Y. Li, S. Liu, et al., Acs Appl Mater Inter 8 (2016) 23533-23541.

[92] Z.M. Zhang, Y. Pan, Y.N. Fang, et al., Nanoscale 8 (2016) 500-507.

[93] H. Feng, Z.Q. Zhang, Q.T. Meng, et al., Advanced Science 5 (2018).

[94] V.-Q. Hieu, M.S. Vinding, M. Jakobsen, et al., Sci Rep-Uk 9 (2019).

[95] C.G. Borrero, J.M. Mountz, J.D. Mountz, Nat Rev Rheumatol 7 (2011) 85-95.

[96] S. Skeoch, H. Williams, P. Cristinacce, et al., Lancet 385 Suppl 1 (2015) S91.

[97] H.J. Kim, S.M. Lee, K.H. Park, et al., Biomaterials 61 (2015) 95-102.

[98] Y. Shi, F. Xie, P. Rao, et al., J Control Release 320 (2020) 304-313.

[99] L. Liu, F.L. Hu, H. Wang, et al., Acs Nano 13 (2019) 5036-5048.

[100] C.Y. Zhao, R. Zhang, Y.W. Luo, et al., Ultrasound Med Biol 46 (2020) 2400-2411.

[101] Z. Chen, Z. Liu, Z. Li, et al., Biomaterials 39 (2015) 15-22.

[102] K. Wang, H.L. Zhang, A.J. Shen, et al., Biomaterials 232 (2020).

[103] Y.S. Chen, S.J. Yoon, W. Frey, et al., Nat Commun 8 (2017).

[104] A. Wang, L. Yin, L. He, et al., Nanoscale 10 (2018) 20126-20130.

[105] M. Bouche, M. Puhringer, A. Iturmendi, et al., Acs Appl Mater Inter 11 (2019) 28648-28656.

[106] H.Z. Guo, S. Song, T.T. Dai, et al., Acs Appl Mater Inter 12 (2020) 17302-17313.

[107] L.K. Prasad, H. O'Mary, Z.R. Cui, Nanomedicine-Uk 10 (2015) 2063-2074.

[108] X. Feng, M. Yang, J. Ding, Austin Arthritis 2 (2017) 1015.

[109] Z.M. Zhang, Y.P. Shi, Y. Pan, et al., J Mater Chem B 2 (2014) 5020-5027.

[110] Y.P. Shi, Z.H. Chen, X. Cheng, et al., Biosens Bioelectron 61 (2014) 397-403.

[111] Y. Pan, Y.P. Shi, Z.H. Chen, et al., Acs Appl Mater Inter 8 (2016) 9472-9482.

[112] Y.P. Shi, C.Q. Yi, Z.M. Zhang, et al., Acs Appl Mater Inter 5 (2013) 6494-6501.

[113] W.D. Chen, Q. Wang, J.P. Ma, et al., Microchim Acta 185 (2018).

[114] W. Ulbrich, A. Lamprecht, J R Soc Interface 7 (2010) S55-S66.

[115] H.W. Ren, Y.W. He, J.M. Liang, et al., Acs Appl Mater Inter 11 (2019) 20304-20315.

[116] K. Coppieters, T. Dreier, K. Silence, et al., Arthritis Rheum 54 (2006) 1856-1866.

[117] M. Higaki, T. Ishihara, N. Izumo, et al., Annals of the Rheumatic Diseases 64 (2005) 1132-1136.

[118] W.U. Kim, W.K. Lee, J.W. Ryoo, et al., Arthritis Rheum 46 (2002) 1109-1120.

[119] W.K. Lee, J.Y. Park, S. Jung, et al., J Control Release 105 (2005) 77-88.

[120] Z.J. Fan, J. Li, J.L. Liu, et al., Acs Appl Mater Inter 10 (2018) 23595-23604.

[121] L.D. Quan, Y.J. Zhang, B.J. Crielaard, et al., Acs Nano 8 (2014) 458-466.

[122] Q. Wang, J.Y. Jiang, W.F. Chen, et al., J Control Release 230 (2016) 64-72.

[123] M.D. Yang, J.X. Ding, Y. Zhang, et al., J Mater Chem B 4 (2016) 2102-2113.

[124] Y.S. Jung, W. Park, K. Na, J Control Release 171 (2013) 143-151.

[125] R.M. Samarasinghe, R.K. Kanwar, J.R. Kanwar, Biomaterials 35 (2014) 7522-7534.

[126] H.F. Zhou, H.M. Yan, Y. Hu, et al., Acs Nano 8 (2014) 7305-7317.

[127] H.F. Zhou, H.M. Yan, A. Senpan, et al., Biomaterials 33 (2012) 8632-8640.

[128] J.M. Metselaar, W.B. van den Berg, A.E.M. Holthuysen, et al., Annals of the Rheumatic Diseases 63 (2004) 348-353.

[129] J.C. Fernandes, H.J. Wang, C. Jreyssaty, et al., Mol Ther 16 (2008) 1243-1251.

[130] G. Courties, M. Baron, J. Presumey, et al., Arthritis Rheum 63 (2011) 681-690.

[131] R.X. Zhang, X.J. Li, L.Y. Qiu, et al., J Control Release 116 (2006) 322-329.

[132] R. Heo, D.G. You, W. Um, et al., Biomaterials 131 (2017) 15-26.

[133] J. Kim, H.Y. Kim, S.Y. Song, et al., Acs Nano 13 (2019) 3206-3217.

[134] T.P. Thomas, S.N. Goonewardena, I.J. Majoros, et al., Arthritis Rheum 63 (2011) 2671-2680.

[135] S.M. Lee, H.J. Kim, Y.J. Ha, et al., Acs Nano 7 (2013) 50-57.

[136] Q.Z. Zhang, D. Dehaini, Y. Zhang, et al., Nat Nanotechnol 13 (2018) 1182.

[137] M.J. Kim, J.S. Park, S.J. Lee, et al., J Control Release 216 (2015) 140-148.

[138] J.M. Metselaar, M.H. Wauben, J.P. Wagenaar-Hilbers, et al., Arthritis Rheum 48 (2003) 2059-2066.

[139] C.H. Li, H.M. Li, Q. Wang, et al., J Control Release 246 (2017) 133-141.

[140] S.J. Lee, A. Lee, S.R. Hwang, et al., Mol Ther 22 (2014) 397-408.

[141] M. Khoury, P. Louis-Plence, V. Escriou, et al., Arthritis Rheum 54 (2006) 1867-1877.

[142] S.I. Simoes, T.C. Delgado, R.M. Lopes, et al., J Control Release 103 (2005) 419-434.

[143] H. Lee, M.Y. Lee, S.H. Bhang, et al., Acs Nano 8 (2014) 4790-4798.

[144] R. Heo, J.S. Park, H.J. Jang, et al., J Control Release 192 (2014) 295-300.

[145] J.S. Smolen, R. Landewe, J. Bijlsma, et al., Ann Rheum Dis 76 (2017) 960-977.

[146] M.P. Venkatesh, P.K. Liladhar, T.M.P. Kumar, et al., Current Drug Therapy 6 (2011) 213-222.

[147] Q.F. Ban, T. Bai, X. Duan, et al., Biomater Sci-Uk 5 (2017) 190-210.

[148] F. Schmitt, L. Lagopoulos, P. Kauper, et al., J Control Release 144 (2010) 242-250.

[149] Y. Lu, L.H. Li, Z.F. Lin, et al., Advanced Healthcare Materials 7 (2018).

[150] A. Singh, Y.H. Seo, C.K. Lim, et al., Acs Nano 9 (2015) 9906-9911.

[151] P.K. Pandey, R. Maheshwari, N. Raval, et al., J Colloid Interf Sci 544 (2019) 61-77.

[152] Q. Tang, J.Y. Cui, Z.H. Tian, et al., Int J Nanomed 12 (2017) 381-393.

[153] S.C. Zhang, L. Wu, J. Cao, et al., Colloid Surface B 170 (2018) 224-232.

[154] C. Hendrich, G. Huttmann, J.L. Vispo-Seara, et al., Knee Surg Sport Tr A 8 (2000) 190-194.

[155] Y.P. Li, T.Y. Lin, Y. Luo, et al., Nat Commun 5 (2014).

[156] S. Bagdonas, G. Kirdaite, G. Streckyte, et al., Photoch Photobio Sci 4 (2005) 497-502.

[157] C.Q. Zhao, F.U. Rehman, Y.L. Yang, et al., Sci Rep-Uk 5 (2015).

[158] C.Q. Zhao, F.U. Rehman, H. Jiang, et al., Sci China Chem 59 (2016) 637-642.

[159] E. Torikai, Y. Kageyama, E. Kohno, et al., Clinical Rheumatology 27 (2008) 751-761.

[160] S. Pervaiz, M. Olivo, Clin Exp Pharmacol P 33 (2006) 551-556.

[161] A. Hansch, O. Frey, M. Gajda, et al., Laser Surg Med 40 (2008) 265-272.

[162] Q. Chen, H.T. Ke, Z.F. Dai, et al., Biomaterials 73 (2015) 214-230.

[163] H.S. El-Sawy, A.M. Al-Abd, T.A. Ahmed, et al., Acs Nano 12 (2018) 10636-10664.

[164] M.H. Lee, E.J. Kim, H. Lee, et al., J Am Chem Soc 138 (2016) 16380-16387.

[165] M.R.I. Shishir, N. Karim, V. Gowd, et al., Trends Food Sci Tech 85 (2019) 177-200.

[166] K. Zhang, Y.D. Zhang, X.D. Meng, et al., Biomaterials 185 (2018) 301-309.

[167] Q. Sun, Q. You, J.P. Wang, et al., Acs Appl Mater Inter 10 (2018) 1963-1975.

[168] Y.N. Dai, J.Z. Su, K. Wu, et al., Acs Appl Mater Inter 11 (2019) 10540-10553.

[169] M.S. Muthu, S.S. Feng, Expert Opin Drug Del 10 (2013) 151-155.

[170] Z. Gan, H. Wu, H.H. Wu, et al., Nan Fang Yi Ke Da Xue Xue Bao 37 (2017) 1283-1289.

[171] Z.P. Xu, Q.H. Zeng, G.Q. Lu, et al., Chem Eng Sci 61 (2006) 1027-1040.

[172] Y. Kumari, G. Kaur, R. Kumar, et al., Advances in Colloid and Interface Science 274 (2019).

[173] S.A. Costa Lima, S. Reis, Colloid Surface B 133 (2015) 378-387.

[174] S.R. Grobmyer, N. Iwakuma, P. Sharma, et al., Methods Mol Biol 624 (2010) 1-9.

[175] S.H. Medina, M.E.H. El-Sayed, Chem Rev 109 (2009) 3141-3157.

[176] S. Parveen, R. Misra, S.K. Sahoo, Nanomedicine-Uk 8 (2012) 147-166.

[177] Y. Kim, E.J. Park, D.H. Na, Archives of Pharmacal Research 41 (2018) 571-582.

[178] M. Krieger, J. Herz, Annu Rev Biochem 63 (1994) 601-637.

[179] M. Zhao, D.A. Beauregard, L. Loizou, et al., Nature Medicine 7 (2001) 1241-1244.

[180] M. Mahmoudi, S. Sant, B. Wang, et al., Adv Drug Deliver Rev 63 (2011) 24-46.

[181] J. Albuquerque, C.C. Moura, B. Sarmento, et al., Molecules 20 (2015) 11103-11118.

[182] S. Sun, J.Q. Chen, K. Jiang, et al., Acs Appl Mater Inter 11 (2019) 5791-5803.

[183] Q.Y. Jia, J.C. Ge, W.M. Liu, et al., Advanced Materials 30 (2018).

[184] Q.Y. Jia, X.L. Zheng, J.C. Ge, et al., J Colloid Interf Sci 526 (2018) 302-311.

[185] Y. Madav, K. Barve, B. Prabhakar, Eur J Pharm Sci 145 (2020) 105240-105240.